Department of Micro- and Nanosciences

Copper-related light-induced degradation in crystalline silicon

Jeanette Lindroos

Aalto University

DOCTORAL DISSERTATIONS

Aalto University publication series
DOCTORAL DISSERTATIONS 37/2015

Copper-related light-induced degradation in crystalline silicon

Jeanette Lindroos

A doctoral dissertation completed for the degree of Doctor of Science (Technology) to be defended, with the permission of the Aalto University School of Electrical Engineering, at a public examination held at the lecture hall E of the school on 24 April 2015 at 12.

Aalto University
School of Electrical Engineering
Department of Micro- and Nanosciences
Electron Physics Group

Supervising professor
Assistant Professor Hele Savin

Preliminary examiners
Professor Michael Seibt, University of Göttingen, Germany
Associate Professor Daniel Macdonald, Australian National University, Australia

Opponent
Professor Eicke Weber, University of Freiburg, Germany

Aalto University publication series
DOCTORAL DISSERTATIONS 37/2015

© Jeanette Lindroos

ISBN 978-952-60-6129-0 (printed)
ISBN 978-952-60-6130-6 (pdf)
ISSN-L 1799-4934
ISSN 1799-4934 (printed)
ISSN 1799-4942 (pdf)
http://urn.fi/URN:ISBN:978-952-60-6130-6

Unigrafia Oy
Helsinki 2015

Finland

Aalto University

Aalto University, P.O. Box 11000, FI-00076 Aalto www.aalto.fi

Abstract

Author
Jeanette Lindroos

Name of the doctoral dissertation
Copper-related light-induced degradation in crystalline silicon

Publisher School of Electrical Engineering

Unit Department of Micro- and Nanosciences

Series Aalto University publication series DOCTORAL DISSERTATIONS 37/2015

Field of research Semiconductor Technology

Manuscript submitted 31 October 2014 **Date of the defence** 24 April 2015

Permission to publish granted (date) 29 January 2015 **Language** English

☐ **Monograph** ☒ **Article dissertation (summary + original articles)**

Abstract

Unintentional copper and nickel impurities are common in silicon-based devices due to the abundance of contamination sources in industrial silicon crystallization and wafer processing lines. High solubility and diffusivity result readily in significant impurity concentrations, which cause charge-carrier recombination and reduce the device response. This work confirms that nickel diffuses as fast as copper in silicon, emphasizing the importance of contamination control in silicon-based devices.

Copper contamination is known to form recombination-active defects in silicon during illumination, which is observed as copper-related light-induced degradation (Cu-LID). In order to identify the extent of degradation in silicon-based devices, this work focuses on determining the properties of Cu-LID in gallium-doped Czochralski (Cz) silicon, boron-doped Cz-Si, and boron-doped multicrystalline silicon. Cu-LID is determined to be predominantly a bulk recombination effect, and the formed defects are found to be stable at 200°C. Slower Cu-LID is observed in Ga-Si compared to B-Si, suggesting that Cu-LID formation is limited by the effective copper diffusivity.

Cu-LID is shown to completely disappear after negative sample surface charging and illumination. The negative surface charge is achieved by corona charging or aluminum oxide deposition. Cu-LID removal is observed to have no impact on classical boron-oxygen-related light-induced degradation (BO-LID), which has previously been shown to recover at 200°C. Unlike BO-LID, the activation energy of Cu-LID is found to depend on the silicon doping concentration. Hence, Cu-LID and BO-LID are concluded to be two different degradation effects, which can occur simultaneously in silicon-based devices.

Keywords copper, degradation, lifetime, nickel, silicon

ISBN (printed) 978-952-60-6129-0 **ISBN (pdf)** 978-952-60-6130-6

ISSN-L 1799-4934 **ISSN (printed)** 1799-4934 **ISSN (pdf)** 1799-4942

Location of publisher Helsinki **Location of printing** Helsinki **Year** 2015

Pages 124 **urn** http://urn.fi/URN:ISBN:978-952-60-6130-6

A? **Aalto-universitetet**

Sammandrag

Aalto-universitetet, PB 11000, 00076 Aalto www.aalto.fi

Författare
Jeanette Lindroos

Doktorsavhandlingens titel
Kopparrelaterad fotodegradering i kristallint kisel

Utgivare Högskolan för elektroteknik

Enhet Institutionen för mikro- och nanoteknik

Seriens namn Aalto University publication series DOCTORAL DISSERTATIONS 37/2015

Forskningsområde Halvledarteknologi

Inlämningsdatum för manuskript 31.10.2014 **Datum för disputation** 24.04.2015

Beviljande av publiceringstillstånd (datum) 29.01.2015 **Språk** Engelska

☐ **Monografi** ☒ **Sammanläggningsavhandling (sammandrag plus separata artiklar)**

Sammandrag

Kiselbaserade elektroniska komponenter är ofta oavsiktligt förorenade av koppar och nickel från otaliga kontaminationskällor i industriella komponentframställningsprocesser. Metallernas höga diffusivitet samt löslighet leder fort till markanta orenhetskoncentrationer, vilka förorsakar rekombination av laddningsbärare och nedsatt komponentrespons. Denna avhandling bekräftar att nickel diffuserar lika fort som koppar i kristallint kisel, vilket betonar vikten av metallorenhetskontroll i kiselbaserade komponenter.

Kopparorenheter förorsakar fotodegradadering (Cu-LID) i kisel via formationen av rekombinationsaktiva koppardefekter under illuminering. För att fastställa omfattningen av fotodegradadering i kiselbaserade komponenter, fokuserar denna avhandling på att identifiera egenskaper för Cu-LID i gallium-dopat Czochralski (Cz) kisel, boron-dopat Cz-Si och boron-dopat mångkristallint kisel. Cu-LID finnes orsaka främst bulkrekombination och de formade koppardefekterna är stabila i 200°C. Cu-LID sker långsammare i Ga-Si jämfört med B-Si, vilket antyder att fotodegraderingsprocessen begränsas av den effektiva koppardiffusiviteten.

I avhandlingen förhindras kopparrelaterad fotodegradadering fullständigt genom att kombinera negativ kiselytladdning med illuminering. Den negativa ytladdningen skapas via deposition av koronaladdning eller aluminiumoxidtunnfilm. Avlägsning av Cu-LID inverkar inte på klassisk bor-syre-relaterad fotodegraderingen (BO-LID), som förekommer i kisel utan kopparföroreningar och försvinner i 200°C. I motsats till BO-LID beror aktiveringsenergin för Cu-LID på dopingkoncentrationen i kiselmaterialet. Följaktligen fastställs Cu-LID och BO-LID vara två skilda former av fotodegradering, vilka kan förkomma samtidigt i kiselbaserade elektroniska komponenter.

Nyckelord degradering, kisel, koppar, livstid, nickel

ISBN (tryckt) 978-952-60-6129-0 **ISBN (pdf)** 978-952-60-6130-6

ISSN-L 1799-4934 **ISSN (tryckt)** 1799-4934 **ISSN (pdf)** 1799-4942

Utgivningsort Helsingfors **Tryckort** Helsingfors **År** 2015

Sidantal 124 **urn** http://urn.fi/URN:ISBN:978-952-60-6130-6

Preface

The research reported in this dissertation was carried out at the Department of Micro- and Nanosciences at Aalto University School of Electrical Engineering (formerly Helsinki University of Technology) and the Department of Mechanical Engineering at Massachusetts Institute of Technology. I would like to express my considerable gratitude to my supervisor Prof. Hele Savin for her patient advice and guidance throughout the past five years. I would like to sincerely thank Prof. Emer. Pekka Kuivalainen for taking me on as a doctoral candidate and Prof. Tonio Buonassisi for an unforgettable year at MIT.

I wish to thank my co-authors for their contribution and pleasant collaboration. I am particularly grateful for the insight and experience of Dr. Marko Yli-Koski and Dr. Antti Haarahiltunen. I thank Dr. Matthias Wagner and the SolarWorld Innovations staff for performing TXRF measurements and providing crucial results critique. I wish to express my gratitude to the members of the Electron Physics Group and the Photovoltaic Research Laboratory for all their help and support, and for showing me that nothing is impossible.

This dissertation was completed thanks to the generous financial support of Aalto University, the Ernst Wirtzen Fund, the Federation of Finnish Technology Industries, the Finnish Cultural Foundation, the Finnish Society of Electronics Engineers, Fortum Foundation, the Fulbright Center, the Swedish Academy of Engineering Sciences in Finland (STViF), and Walter Ahlström Foundation. The research materials were funded through several projects supported by the Academy of Finland, Beneq Oy, Epicrystals Oy, the European Research Council, the Finnish Funding Agency for Technology and Innovation (TEKES), Fortum Oyj, Luvata Pori Oy, Okmetic Oyj, Semilab Inc., SolarWorld Innovations GmbH, and the U.S. Department of Energy.

I would like to acknowledge the Aalto Nanofab staff for their commitment to cleanroom cleanliness and equipment maintenance. Finally, I wish to thank my family and friends for all their support and encouragement throughout my doctoral studies.

Karlstad, Sweden, March 16, 2015,

Jeanette Lindroos

Contents

Preface 1

Contents 3

List of Publications 5

Author's Contribution 7

List of Abbreviations 9

List of Symbols 11

1. Introduction 13

2. Fast-Diffusing Transition Metals 15

2.1 Copper 15

2.1.1 Diffusivity and solubility 15

2.1.2 Point defects and complexes 16

2.1.3 Precipitates 18

2.1.4 Low-temperature stability 19

2.2 Nickel 20

2.2.1 Diffusivity and solubility 20

2.2.2 Point defects and complexes 21

2.2.3 Precipitates 22

3. Light-Induced Degradation 23

3.1 Boron-oxygen degradation 23

3.1.1 Degradation rate 24

3.1.2 Activation energy 25

3.1.3 Metastable defect 26

3.1.4 Mitigating degradation 27

3.1.5 Multicrystalline silicon . . . 28
3.2 Copper-related degradation . . . 28
3.2.1 Degradation rate and defect density . . . 28
3.2.2 Copper-related defect . . . 30
3.2.3 Mitigating copper . . . 32

4. Results and Discussion **35**
4.1 Materials affected by copper-related LID . . . 35
4.2 Bulk versus surface LID . . . 36
4.2.1 Surface passivation stability . . . 36
4.2.2 Copper-related LID . . . 39
4.3 Impact of doping on copper-related LID . . . 40
4.4 Temperature dependence of copper-related LID . . . 42
4.5 Low-temperature stability . . . 44
4.5.1 Before illumination . . . 44
4.5.2 After illumination . . . 45
4.6 Mitigating copper-related LID . . . 45
4.6.1 Negative corona charging . . . 45
4.6.2 Aluminum oxide . . . 50
4.6.3 Phosphorus diffusion gettering . . . 50
4.7 Copper-related LID compared with boron-oxygen LID . . . 51
4.8 Nickel diffusivity compared with copper diffusivity . . . 52

5. Conclusions **55**

References **57**

Errata **73**

Publications **75**

List of Publications

This thesis consists of an overview and of the following publications which are referred to in the text by their Roman numerals.

I J. Lindroos, M. Yli-Koski, A. Haarahiltunen, M. C. Schubert, and H. Savin, Light-induced degradation in copper-contaminated gallium-doped silicon, *Physica Status Solidi - Rapid Research Letters* 7, No. 4, p. 262-264 (2013).

II J. Lindroos, M. Yli-Koski, A. Haarahiltunen, and H. Savin, Room-temperature method for minimizing light-induced degradation in crystalline silicon, *Applied Physics Letters* 101, 232108 (2012).

III Y. Boulfrad, J. Lindroos, Mt. Wagner, F. Wolny, M. Yli-Koski, and H. Savin, Experimental evidence on removing copper and light-induced degradation from silicon by negative charge, *Applied Physics Letters* 105, 182108 (2014).

IV J. Lindroos and H. Savin, Formation kinetics of copper-related light-induced degradation in crystalline silicon, *Journal of Applied Physics* 116, 234901 (2014).

V J. Lindroos, Y. Boulfrad, M. Yli-Koski, and H. Savin, Preventing light-induced degradation in multicrystalline silicon, *Journal of Applied Physics* 115, 154902 (2014).

VI J. Lindroos, D. P. Fenning, D. J. Backlund, E. Verlage, A. Gorgulla, S. K. Estreicher, H. Savin, and T. Buonassisi, Nickel: A very fast diffuser in silicon, *Journal of Applied Physics* 113, 204906 (2013).

Author's Contribution

Publication I: "Light-induced degradation in copper-contaminated gallium-doped silicon"

The author participated actively in experiment planning, sample processing, and lifetime measurements. The author prepared the manuscript.

Publication II: "Room-temperature method for minimizing light-induced degradation in crystalline silicon"

The author processed the samples, performed all measurements, and prepared the manuscript.

Publication III: "Experimental evidence on removing copper and light-induced degradation from silicon by negative charge"

The author participated actively in experiment planning, lifetime measurements, and manuscript writing.

Publication IV: "Formation kinetics of copper-related light-induced degradation in crystalline silicon"

The author planned and performed all experiments, and prepared the manuscript.

Publication V: "Preventing light-induced degradation in multicrystalline silicon"

The author performed experiment planning, sample processing, lifetime measurements, and manuscript preparation.

Publication VI: "Nickel: A very fast diffuser in silicon"

The author participated actively in experiment planning and sample preparation. The author performed the XRF measurements and prepared the manuscript.

List of Abbreviations

A center	Oxygen-vacancy complex
Al	Aluminum
ALD	Atomic Layer Deposition
Al_2O_3	Aluminum oxide
B	Boron
B_i	Interstitial boron
B_s	Substitutional boron
BMD	Bulk micro-defect
BO	Boron-oxygen complex
BO-LID	Boron-oxygen light-induced degradation
CH_3COOH	Acetic acid
CO_3^-	Negative corona charge
Cu	Copper
Cu_i	Interstitial copper
Cu_s	Substitutional copper
CuAl	Copper-aluminum pair
CuB	Copper-boron pair
CuGa	Copper-gallium pair
CuIn	Copper-indium pair
Cu_3Si	Copper precipitate, copper silicide
Cu_sCu_i	Substitutional and interstitial copper pair
$Cu_{s1}Cu_{i3}$	Substitutional and interstitial copper complex
Cu-LID	Copper-related light-induced degradation
Cz-Si	Czochralski silicon
DLTS	Deep-Level Transient Spectroscopy
FeB	Iron-boron pair
FRC	Fast recombination center
FZ-Si	Float Zone silicon
Ga	Gallium

Ga_s	Substitutional gallium
H	Hydrogen
HF	Hydrofluoric acid
HNO_3	Nitric acid
H_3O^+	Positive corona charge
In	Indium
IR	Infrared
LID	Light-induced degradation
mc-Si	Multicrystalline silicon
MCz-Si	Magnetic Czochralski silicon
μ-PCD	Microwave Photoconductance Decay
NAA	Neutron Activation Analysis
NEB	Nudged Elastic Band
Ni	Nickel
Ni_i	Interstitial nickel
Ni_s	Substitutional nickel
$NiSi_2$	Nickel precipitate, nickel silicide
O	Oxygen
O_i	Interstitial oxygen
O_{2i}	Oxygen dimer
P	Phosphorous
PDG	Phosphorus diffusion gettering
PL	Photoluminescence
ppm	Parts per million
QSSPC	Quasi-Steady-State Photoconductance Decay
RBS	Rutherford Backscattering
RT	Room temperature
Si	Silicon
SiO_2	Silicon dioxide
SRC	Slow recombination center
SRH	Shockley-Read-Hall
TID	Transient Ion Drift
TXRF	Total Reflection X-Ray Fluorescence
UMG-Si	Upgraded metallurgical grade silicon
UV	Ultraviolet
V	Vacancy

List of Symbols

a	Degradation fitting parameter
b	Degradation fitting parameter
c	Degradation fitting parameter
C_{Cu}	Dissolved copper concentration
C_{Ni}	Dissolved nickel concentration
d	Degradation fitting parameter
d_{Si}	Wafer thickness
$D_{\mathrm{Cu,eff}}$	Effective copper diffusivity
$D_{\mathrm{Cu,in}}$	Intrinsic copper diffusivity
D_{Ni}	Nickel diffusivity
D_{it}	Interface defect density
E_{C}	Energy level of conduction band edge
E_{def}	Defect formation energy
E_{Fn}	Quasi-Fermi level of electrons
E_{Fp}	Quasi-Fermi level of holes
E_{V}	Energy level of valence band edge
J_{Ni}	Nickel flux
k	Degradation fitting parameter
k_B	Boltzmann constant
n	Copper precipitate density
N_{A}	Acceptor concentration
N_{D}	Donor concentration
N_t	Defect density
N_{t}^*	Normalized defect density
$N_{\mathrm{t}}^*(\infty)$	Saturated normalized defect density
p_0	Equilibrium hole concentration
r	Copper precipitate radius

R	Recombination rate
R_{def}	Degradation rate
R_{SRC}	Degradation rate of the slow recombination center
S_{Cu}	Copper solubility
S_{Ni}	Nickel solubility
t	Time
t_{ox}	Silicon dioxide thickness
T	Temperature
W	Depletion width

Δn	Excess electron concentration
η	Injection level
κ_0	Pre-exponential of defect formation
μ	Chemical precipitation force
ν_n	Mean thermal electron velocity
σ_n	Defect electron-capture cross-section
σ_p	Defect hole-capture cross-section
τ_{def}	Degradation time constant
τ_{Aug}	Auger recombination lifetime
τ_{eff}	Effective recombination lifetime
τ_{n}	Electron lifetime
τ_{rad}	Radiative recombination lifetime
τ_{s}	Surface recombination lifetime
τ_{SRH}	Shockley-Read-Hall recombination lifetime
ϕ_{s}	Surface potential

1. Introduction

Copper and nickel are common metal impurities in silicon, as unintentional contamination can easily occur during different steps of silicon-based device processing.[1] Copper and nickel can diffuse from the quartz crucible into the silicon bulk already during ingot growth.[2–4] Silicon surface contamination may occur, *e.g.*, from sawing wires during wafering,[5] steel parts or gas supply systems during processing,[1] and device metallization. Surface copper and nickel contamination is difficult to remove with standard wafer cleaning or silicon etching, as both metals replate to the wafer surface during wet chemical processing.[1,6] Subsequent processing at elevated temperature turns surface copper and nickel contamination easily into a variety of recombination-active bulk defects, due to their high diffusivity and solubility in silicon.[7]

Interstitial copper was presumed harmless in boron-doped Czochralski-grown (Cz) silicon, until Henley et al.[8] observed copper-related recombination during illumination in 1998. The effect is known as copper-related light-induced degradation (Cu-LID), but the specific recombination-active defect formed during illumination remains to be determined. The proposed copper-related defects are substitutional copper,[8,9] copper precipitates,[10,11] and copper-related Si/SiO_2 interface defects.[12]

Light-induced degradation (LID) is also used to describe a 1-2% absolute efficiency loss observed in Cz-Si solar cells during one day of illumination.[13,14] LID is seen as a short-circuit current decrease and an open-circuit voltage loss, caused by a minority-carrier recombination increase in the B-doped bulk. Although Fischer and Pschunder[15] first observed LID in 1973, the defect responsible for LID remains unknown. Most studies refer to a boron-oxygen (BO) complex, as LID detection requires both high boron and oxygen concentrations, prompting the term boron-oxygen LID (BO-LID).[16] However, Möller and Lauer[17,18] have observed LID in

aluminum-doped and indium-doped Cz-Si, suggesting LID to be caused by the formation of an acceptor and silicon self-interstitial pair.

Recently, some multicrystalline (mc) silicon materials have also exhibited stronger LID than predicted by BO-LID theory.[14, 19–21] Since mc-Si is known to contain relatively high concentrations of transition metals,[3] the stronger LID might be linked to copper-related degradation. Therefore, this dissertation aims to determine the extent and properties of copper-related light-induced degradation in crystalline silicon. The extent of Cu-LID is examined in different silicon materials in Publications I, IV, and V. The formation kinetics of Cu-LID are investigated in Publications I-V, in order to determine whether Cu-LID and BO-LID are related effects. Cu-LID is mainly characterized by minority-carrier recombination lifetime methods in Publications I-V, but chemical analysis is also performed with Total Reflection X-Ray Fluorescence (TXRF) in Publication III. By applying copper removal techniques, the goal is to develop a method for Cu-LID prevention in Publications II, III, IV, and V. Although interstitial nickel shows no light sensitivity, the final aim in Publication VI is to determine whether nickel diffuses as fast copper in silicon.

Chapter 2 compiles literature results on copper and nickel properties in silicon, while Chapter 3 reviews previous studies on boron-oxygen LID and copper-related LID in crystalline silicon and silicon solar cells. Chapter 4 summarizes new results obtained on copper-related LID and nickel diffusivity in Publications I-VI. Chapter 5 presents the final conclusions together with recommendations for further work.

2. Fast-Diffusing Transition Metals

Copper and nickel are $3d$ transition metals with high diffusivity and solubility in crystalline silicon.[7] Both metals form several defects with deep energy levels in the silicon bandgap, causing Shockley-Read-Hall (SRH) recombination.[22,23] At low injection levels, the SRH recombination lifetime can be approximated by the minority carrier recombination lifetime.[24] This chapter compiles literature results on copper and nickel properties in crystalline silicon with a focus on boron-doped silicon.

2.1 Copper

2.1.1 Diffusivity and solubility

Copper diffuses interstitially in silicon as a positively charged ion Cu_i^+.[7,25] Copper diffusivity in intrinsic and n-type Si has been determined with Transient Ion Drift (TID) as[26]

$$D_{\mathrm{Cu,in}}(T) = (3.0 \pm 0.3) \times 10^{-4} \exp(-0.18 \pm 0.01\,\mathrm{eV}/k_B T)\ \mathrm{cm^2 s^{-1}}\,, \quad (2.1)$$

where k_B is Boltzmann constant and T is the temperature in K. The measured activation energy of 0.18 eV matches the most recent first-principles calculations[27] obtained with the Nudged Elastic Band (NEB)[28–31] method.

In p-type Si, interstitial copper forms neutral pairs with negatively charged acceptor atoms, such as CuB, CuGa, CuAl, and CuIn. Pair formation decreases the density of mobile copper ions, decreasing the effective diffusivity of copper. Copper diffusion has been shown to be faster in B-doped than in Ga-doped silicon due to the lower dissociation energy of CuB (0.61 ± 0.02 eV) compared to CuGa (0.71 ± 0.02 eV).[26,32] The dissociation energy of CuAl and CuIn has been measured as 0.70 eV.[32] In B-doped silicon with a doping concentration below 10^{17} cm^{-3}, the effective diffusiv-

ity $D_{\mathrm{Cu,eff}}$ has been measured as[26]

$$D_{\mathrm{Cu,eff}}(T) = \frac{3\times10^{-4}\exp(-2090/T)}{1+2.584\times10^{-20}\exp(4990/T)(N_{\mathrm{A}}/T)}\ \mathrm{cm^2s^{-1}}\,, \tag{2.2}$$

where N_{A} is the acceptor concentration, and when $-33<T<107$°C. Even though the boron doping decreases the diffusivity, CuB pairs remain unstable at RT,[26] allowing copper to diffuse through a 400 µm wafer with [B]=4×10^{15} cm^{-3} in less than 11 h. The solubility of interstitial copper has been measured as[7]

$$S_{\mathrm{Cu}}(T) = 5\times10^{22}\exp\left(2.4-\frac{1.49\,\mathrm{eV}}{k_BT}\right)\ \mathrm{cm^{-3}}\,, \tag{2.3}$$

when $500<T<800$°C.

2.1.2 Point defects and complexes

Interstitial copper

Interstitial copper does not cause significant minority carrier recombination in silicon. In B-doped Cz-Si, even a minority-carrier recombination lifetime increase has been measured at $\mathrm{Cu_i^+}$ concentrations below 10^{14} cm^{-2}, although the cause for the increase remains unclear.[33–37] Interstitial copper has been associated with a donor level of $E_{\mathrm{C}}-0.15$ eV, as shown in Fig. 2.1, although the unstable level was only detected in n-Si.[38] The $\mathrm{Cu_i^+}$ level loss was associated with the activation energy of 0.55 ± 0.05 eV, which was presumed to reflect copper precipitate formation.[38]

In bare p-Si, interstitial copper does not stay in the bulk, but diffuses towards the wafer surface in order to reach equilibrium solubility.[39] At RT, such out-diffusion has been observed to occur within a few hours to several days depending on the wafer thickness[40] and the doping[41] concentration. Copper out-diffusion has been slowed down by a 0.2 V surface potential barrier[41] or prevented by a $3-4$ nm surface oxide with a positive charge.[42] Hence, a positive surface potential is thought to repel $\mathrm{Cu_i^+}$, inhibiting copper out-diffusion.

Substitutional copper

Copper can also exist as a recombination-active substitutional impurity in silicon. Interstitial copper becomes $\mathrm{Cu_s}$ by reacting with a vacancy releasing $2.5-2.8$ eV[25,43] or with a Si self-interstitial releasing 1.2 eV.[44] Copper has also been shown to react with the oxygen-vacancy A center according to $\mathrm{Cu_i}+\{\mathrm{O},\mathrm{V}\}\rightarrow\{\mathrm{Cu_s},\mathrm{O_i}\}$ at $175-250$°C, creating a new defect level at $E_{\mathrm{C}}-0.6$ eV.[45]

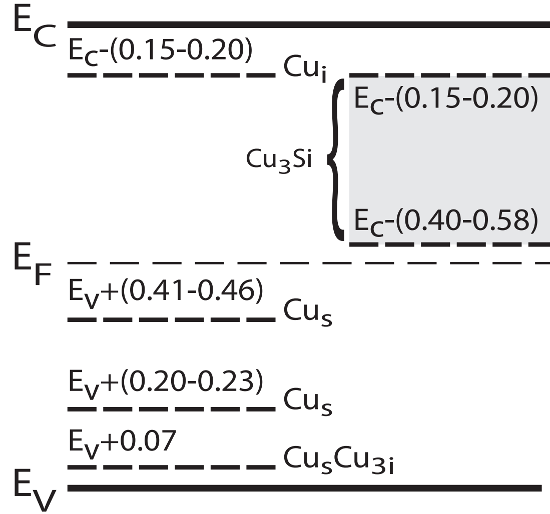

Figure 2.1. Defect energy levels in the silicon bandgap associated with interstitial copper (Cu_i),[38] substitutional copper (Cu_s),[46–54] the copper complex (Cu_sCu_{3i}),[57] and copper precipitates (Cu_3Si).[58–60]

Deep-Level Transient Spectroscopy (DLTS) measurements have associated Cu_s with the two energy levels of E_V+(0.2-0.23) eV ($Cu_s^{+/0}$)[46–53] and E_V+(0.41-0.46) eV ($Cu_s^{0/-}$),[48,50,52–54] as presented in Fig. 2.1. The hole capture cross-sections of the defect levels have been estimated as 3×10^{-14} cm^2 and 1.5×10^{-14} cm^2, respectively.[1] The energy level of $E_C-(0.15\text{-}0.2)$ eV[47,48,50,51,53,55] was originally also associated with Cu_s, until Istratov et al.[38] showed the donor level to be related to interstitial copper. The concentration of Cu_s is usually less than 0.1% of the copper solubility during any high-temperature process.[56]

Copper complexes

Substitutional copper forms several complexes with hydrogen,[44,61,62] while interstitial copper is known to react weakly with oxygen.[44,63] Copper also forms pure copper complexes, which were long presumed to be Cu_sCu_i pairs[64,65] but has now been identified as four copper atom complexes.[66,67] The most likely composition of the pure copper complex is $Cu_{s1}Cu_{i3}$.[62,68,69] DLTS measurements have revealed a copper complex energy level at E_V+ 0.07 eV,[57] and Photoluminescence (PL) has shown a sharp line at 1014 meV.[70] FZ-Si has exhibited a one to two orders of magnitude larger PL signal compared to Cz-Si,[71] which might be due to the higher vacancy concentration in FZ-Si, enabling Cu_s formation. Copper complexes have been observed to form with the activation energy of 0.57 ± 0.05 eV.[72] A complex concentration decrease has been observed at 150°C[73] with full complex

dissociation at 250°C.[57,73]

2.1.3 Precipitates

Interstitial copper precipitates as η''-Cu_3Si in silicon.[74–77] Copper precipitates cause severe minority-carrier recombination, since they form a deep defect band between $E_C-(0.15\text{-}0.2)$ eV and $E_C-(0.4\text{-}0.58)$ eV,[58–60] as shown in Fig. 2.1. The electron capture cross-section of Cu_3Si has been estimated as 3×10^{-16} cm^2.[78] The precipitate size and distribution has been shown to depend on the wafer copper concentration, the doping concentration, the bulk defect concentration, the surface potential, and the thermal history. The chemical precipitation force μ is defined as[58,79]

$$\mu = k_B T \ln\left(\frac{C_{\mathrm{Cu}}}{S_{\mathrm{Cu}}(T)}\right) , \tag{2.4}$$

where C_{Cu} is the dissolved copper concentration and $S_{\mathrm{Cu}}(T)$ is the equilibrium copper solubility in Eq. 2.3. The driving force μ grows during supersaturation, as the dissolved copper concentration C_{Cu} exceeds the equilibrium solubility S_{Cu}. Nevertheless, copper precipitates only when the driving force μ exceeds the precipitation nucleation barrier.[80]

Fast quenching from high temperatures leads to high supersaturation and the formation of homogeneously distributed small copper precipitates.[80] High copper concentrations ($>10^{17}$ cm^{-3}) have shown to form platelet-like precipitates ($30-500$ nm) mostly in the {111} plane up to 10^{13} cm^{-3}.[58,81,82] Slower cooling leads to a lower density of larger precipitate colonies heterogeneously distributed near the sample surface of defect-free Si, known as haze.[81–83] The large lattice mismatch of 150% between Cu_3Si and Si has been observed to cause stacking fault formation during precipitation.[78] As stacking faults provide a low nucleation barrier for copper precipitates, large copper colonies ($0.5-80$ µm)[77] have been shown to consist of copper platelets surrounded by stacking faults with small spherical copper precipitates.[81,82] Heterogeneous copper precipitation does not only form near the surface but also in the mc-Si bulk, which contains significant concentrations of stacking faults, dislocations, and higher sigma grain boundaries with low precipitation barriers.[84] Copper has also been shown to precipitate near oxygen precipitates,[85] suggesting that copper traps at Si self-interstitials formed during oxygen precipitation.[44]

The time and temperature required to dissolve a specific size of copper precipitate can be estimated based on the copper diffusivity and solubil-

ity at the annealing temperature, the precipitate copper concentration, and the sample copper concentration far from the precipitate.[86] Although 45 min at 560°C predicts dissolution of precipitates smaller than 420 nm, only partial dissolution of heterogeneous precipitates has been observed at 360–560°C in Cz-Si with copper concentrations of 10^{16}–10^{17} cm^{-3}.[85,87] Therefore, the dissolution experiments confirm the formation of large copper colonies[77,81,82] during heterogeneous copper precipitation.

Even though the chemical precipitation force at RT can be as high as 0.9 eV,[88] not all copper precipitates in defect-free p-Si.[40,89,90] Therefore, supersaturation has been proven as only one prerequisite for copper precipitation. At RT, copper has been shown to precipitate only when the Fermi level exceeds the Cu_3Si neutrality level of $E_C-0.2$ eV,[40] at which Cu_3Si changes its charge state from positive to neutral or negative. Below $E_C-0.2$ eV, Cu_3Si is shown to be positively charged, repelling positively charged interstitial copper and preventing precipitate growth.[58] In n-Si, the Fermi level exceeds $E_C-0.2$ eV at P doping concentrations above 1.7×10^{16} cm^{-3}, resulting in copper precipitation at 300 K regardless of impurity concentration in typical n-Si. In B-doped Si, Cu_3Si has been shown to reach the neutrality level, only when the copper concentration exceeds the acceptor density by 10^{16} cm^{-3}.[40] Therefore, n-Si is more sensitive to copper contamination than p-Si.[34,36,37] The effect of illumination on the Fermi level and copper precipitation is further discussed in Sec. 3.2.2.

2.1.4 Low-temperature stability

Although some copper stays interstitial in oxidized p-Si at RT,[40] increasing the temperature to 75°C has been observed to impact the minority-carrier diffusion length.[9,91] After 30 min at 75°C, Ramappa and Henley have observed a diffusion length increase in Cz-Si[91] and a decrease in FZ-Si.[9] As no copper contamination levels were reported, the opposite diffusion length behavior could have been caused by either a difference in the copper concentration[40] or the bulk material. The Cz-Si diffusion length increase was associated with thermal copper precipitation, since Istratov et al.[92] previously suggested copper precipitation as the reason for a Cu_i concentration decrease and a diffusion length increase in p-type FZ-Si at RT. However, Istratov's samples contained a Cu_i concentration lower than the doping level, making copper precipitation at RT less likely than out-diffusion.[40] Annealing above 75°C raises the Fermi level, but not above the precipitate neutrality level of $E_C-0.2$ eV, even in low-resistivity

p-Si. Therefore, the lifetime increase measured by Ramappa and Henley[91] in Cz-Si was probably caused by some other reaction than copper precipitation.

After annealing for 60 min above 100°C, Ramappa and Henley[91] eventually observed a diffusion length decrease also in the Cz-Si material. The diffusion length decrease had an activation energy of 0.419 eV, which was associated with thermal dissociation of copper pairs (Cu_sCu_i) and subsequent release of recombination-active Cu_s.[9] Although the copper pair is now known to be four atom copper complex,[66,67] the complex is still very likely to contain substitutional copper[62,68,69] as discussed in Sec. 2.1.2. However, copper complex dissociation has only been observed above 150°C,[57,73] suggesting the formation of some other copper-related recombination-active defect during 60 min annealing above 100°C.

At 200°C, Cu-Si phase studies have concluded that η''-Cu_3Si begins to form in the interface of bulk silicon and thin-film copper.[93–95] Internal ripening of small homogeneous copper precipitates into larger heterogeneous precipitates has been observed at $260-400$°C.[81,96] Since the thermal stability of several copper-related defect remains unknown, this work further studies the low-temperature behavior of the minority carrier lifetime in copper-contaminated Cz-Si. The main results are presented in Sec. 4.5.

2.2 Nickel

2.2.1 Diffusivity and solubility

Nickel diffuses interstitially in silicon without a charge as Ni_i^0. Due to its charge neutrality, nickel does not form any acceptors or donor pairs as opposed to copper. Therefore, the nickel diffusivity is independent of the doping density. Already in 1964, Yoshida and Furusho[97] estimated a nickel diffusivity of 10^{-4}–10^{-5} cm^{2}s^{-1} at $800-1200$°C. Figure 2.2 depicts the diffusivity data obtained since then,[98–104] including the most frequently cited nickel diffusivity D_{Ni} of[98]

$$D_{\mathrm{Ni}}(T) = 2.3 \times 10^{-3}\exp(-0.47\,\mathrm{eV}/k_BT)\ \mathrm{cm^2s^{-1}}\,, \tag{2.5}$$

when $800<T<1300$°C. However, first principles calculations using the NEB method have resulted in a nickel diffusivity activation energy of 0.21 eV,[27,105] which is less than half of the measured activation energy in Eq. 2.5. At 900°C, the solubility obtained in the same abstract[98] is also four

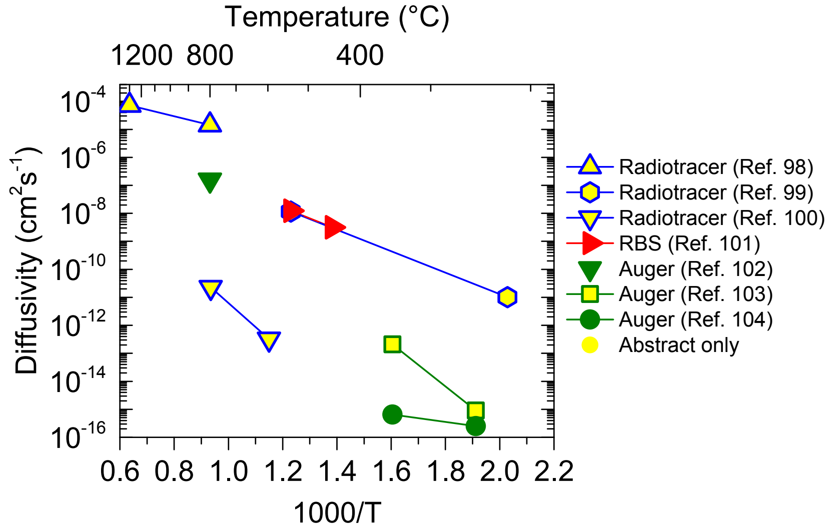

Figure 2.2. Diffusivity of interstitial nickel in silicon obtained by Radiotracer, Rutherford Backscattering (RBS), or Auger spectroscopy.[98–104]

orders of magnitude lower than the literature interstitial nickel solubility S_{Ni} of[106]

$$S_{\mathrm{Ni}}(T) = 1.227 \times 10^{24} \exp(-1.68\,\mathrm{eV}/k_B T)\ \mathrm{cm}^{-3}\,, \tag{2.6}$$

obtained by Neutron Activation Analysis (NAA) and valid for $T<964$°C. These discrepancies raise the need for a re-examination of the interstitial nickel diffusivity. The main results are presented in Sec. 4.8.

2.2.2 Point defects and complexes

Interstitial nickel is not considered recombination active, as no defect level has been observed in the silicon bandgap.[105] However, interstitial nickel is unstable in silicon, as nickel in known to form precipitates, substitutional defects, and different impurity complexes at RT. Figure 2.3 presents nickel-related defect energy levels in the silicon bandgap.

Interstitial nickel becomes $\mathrm{Ni_s}$ by moving into a vacancy, which has been calculated to release 2.6 eV.[105] In p-Si, first principles calculations have predicted a donor level at $E_{\mathrm{V}}+0.30$ eV ($\mathrm{Ni_s^{+/0}}$),[105] while DLTS measurements have yielded two defect levels: $E_{\mathrm{V}}+(0.15\text{-}0.21)$ eV[107–115] and $E_{\mathrm{V}}+(0.31\text{-}0.35)$ eV.[116–119] DLTS measurements in n-Si have revealed two acceptor levels of $E_{\mathrm{C}}-(0.36\text{-}0.47)$ eV[53,107–113,115,120–124] and $E_{\mathrm{C}}-(0.08\text{-}0.21)$ eV,[107,115,120,121] which are similar to the two calculated levels of $E_{\mathrm{C}}-0.31$ eV ($\mathrm{Ni_s^{0/-}}$) and $E_{\mathrm{C}}-0.16$ eV ($\mathrm{Ni_s^{-/--}}$).[105] Although the $\mathrm{Ni_s}$ concentration has been shown to depend on the cooling rate,[119] it has accounted for no

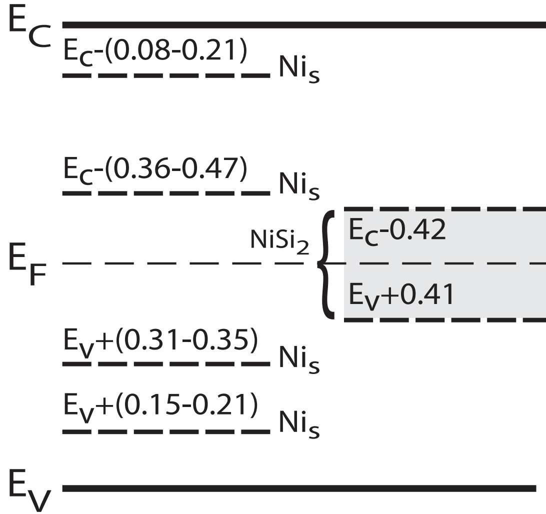

Figure 2.3. Defect energy levels in the silicon bandgap associated with substitutional nickel (Ni_s)[53,107–112,112–118,120–124] and nickel precipitates ($NiSi_2$).[78]

more than 0.1% of the dissolved nickel concentration.[125] DLTS measurements have also resulted in eleven defect levels associated with nickel and hydrogen,[115] although first principles calculations have predicted only two Ni_s-H complexes and no stable Ni_i-H complex.[126]

2.2.3 Precipitates

Similar to copper, supersaturation of dissolved nickel results in nickel precipitation. Rapid quenching has been observed to create platelet-like nickel precipitates ($7-100$ nm) consisting of two {111} layers of $NiSi_2$[127] that are bound by a dislocation.[128] The lattice mismatch between $NiSi_2$ and Si has been determined as 1.2%, which is significant enough to form dislocations but not stacking faults.[78]

During slow cooling of defect-free Si, nickel has been observed to prefer out-diffusion towards the sample surface and precipitation near the surface.[129–132] In the presence of oxygen precipitates, nickel has been shown to precipitate in the bulk regardless of cooling profile.[131,133] Nickel precipitates have been reported to form a defect band between $E_V+0.41$ eV and $E_C-0.42$ eV with an electron-capture cross section of 5×10^{-14} cm^2, as shown in Fig. 2.3.[78] Nickel-related minority-carrier recombination has been observed in n-type[36] Cz-Si at Ni concentrations of 1×10^{11} cm^{-2}, and in p-type[134] at as low as 3×10^{10} cm^{-2}, correspondingly.

3. Light-Induced Degradation

Light-induced degradation (LID) is a deleterious effect in crystalline silicon, which is observed as a minority-carrier recombination lifetime decrease during illumination. In the past four decades, LID has been studied extensively in order to identify the recombination-active defect responsible for the degradation and develop methods for preventing LID. Although several advances have been made in characterizing LID,[135] no agreement exists on its origin.[14,136,137] Most studies point to a boron-oxygen (BO) complex,[16,138] but with no experimental evidence on the existence of such a complex.[139] Others connect the degradation with a recombination-active copper-related defect,[140] but the defect composition remains unknown. Moreover, the analysis of LID often becomes more complex by the presence of light-sensitive iron-boron pairs (FeB)[135] and unstable surface passivation thin films such as aluminum oxide.[141,142]

3.1 Boron-oxygen degradation

In clean Cz-Si with sufficiently high boron and oxygen concentrations,[16] BO-LID is observed during illumination as a fast initial exponential lifetime decay (FRC), followed by a second slower asymptotic degradation (SRC), as shown in Fig. 3.1.[143–146] Photons are not directly involved in the formation of LID, since similar degradation curves has been measured during solar cell forward biasing in the dark.[147] Although LID has been shown to occur at excess-carrier concentrations as low as 1.7×10^9 cm^{-3},[148] the excess carrier concentration does not either explain the extent of LID. In fact, Bothe et al.[149] have shown that BO-LID formation is determined by the *total* number of minority carriers, based on LID observation in the dark at zero bias above 300 K.

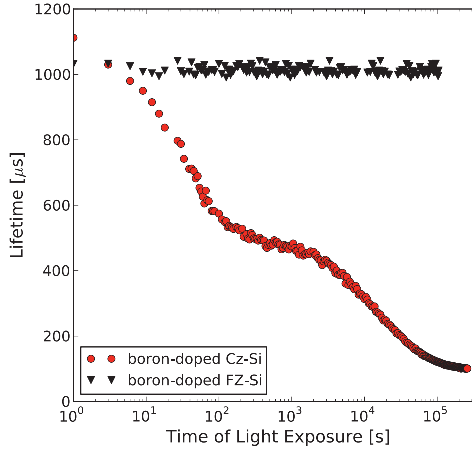

Figure 3.1. Effective minority-carrier recombination lifetime as a function of illumination time in clean low-resistivity boron-doped Cz-Si and FZ-Si.[146] (Reprinted with permission from T. U. Nærland, Characterization of light induced degradation in crystalline silicon, Norwegian University of Science and Technology, Trondheim, Norway, Vol. 2013:303 (2013). Copyright 2013, T. U. Nærland.)

3.1.1 Degradation rate

The degradation rate of the fast (FRC) and the slow (SRC) recombination centers can be obtained by minority-carrier recombination lifetime measurements with Microwave Photoconductance Decay (μ-PCD)[150] and Quasi-Steady-State Photoconductance Decay (QSSPC).[151] The effective recombination lifetime τ_{eff} in Fig. 3.1 is determined by the surface (τ_{s}), the Shockley-Read-Hall (τ_{SRH}), the radiative (τ_{rad}), and the Auger (τ_{Aug}) recombination lifetimes. Radiative recombination is negligible in silicon, and Auger recombination dominates only at high injection levels.[24] At low injection levels in p-Si, the Shockley-Read-Hall recombination lifetime is approximated by the minority carrier recombination lifetime τ_{n}, and the recombination rate R becomes[24]

$$\begin{aligned} R = \frac{\Delta n}{\tau_{\text{eff}}} = \Delta n \left[\frac{1}{\tau_{\text{s}}} + \left(\frac{1}{\tau_{\text{SRH}}} + \frac{1}{\tau_{\text{rad}}} + \frac{1}{\tau_{\text{Auger}}} \right) \right] \approx \\ \approx \Delta n \left[\frac{1}{\tau_{\text{s}}} + \frac{1}{\tau_{\text{n}}} \right] \approx \Delta n \left[\frac{1}{\tau_{\text{s}}} + \sigma_n \nu_n N_t \right], \end{aligned} \tag{3.1}$$

where Δn is the excess electron concentration, σ_n is the LID defect electron-capture cross-section, ν_n is the mean thermal electron velocity, and N_t is the LID defect density. Consequently, the light-induced defect density N_t at illumination time t can be determined from the initial recombination

rate $R(0)$ and the time-dependent rate $R(t)$ in Eq. 3.1 by

$$\begin{aligned} R(t) - R(0) &= \Delta n \left[\frac{1}{\tau_{\text{eff}}(t)} - \frac{1}{\tau_{\text{eff}}(0)} \right] = \\ &= \Delta n \left[\left(\frac{1}{\tau_{\text{s}}(t)} + \frac{1}{\tau_{\text{n}}(t)} \right) - \frac{1}{\tau_{\text{s}}(0)} \right] = \\ &= \frac{\Delta n}{\tau_{\text{n}}(t)} = \Delta n \sigma_n \nu_n N_t(t) \,, \end{aligned} \tag{3.2}$$

when the surface recombination lifetime is constant during illumination ($\tau_{\text{s}}(t)$=$\tau_{\text{s}}(0)$). As the electron-capture cross-section σ_n is unknown, the normalized LID defect density $N_{\text{t}}^*(t)$ is defined as[16]

$$N_{\text{t}}^*(t) = \sigma_n \nu_n N_T = \frac{1}{\tau(t)} - \frac{1}{\tau(0)} \,, \tag{3.3}$$

when the effective lifetimes τ are measured at the same low injection level. In LID studies, effective lifetimes are often reported at the injection level η=$\Delta n/p_0$= 0.1.[137,144] The degradation rate R_{def} and the degradation time constant τ_{def} are then determined by fitting the normalized defect density $N_{\text{t}}^*(t)$ separately to the FRC and the SRC lifetime decays with[16]

$$\begin{aligned} N_{\text{t}}^*(t) = \frac{1}{\tau(t)} - \frac{1}{\tau(0)} &= \left(\frac{1}{\tau(\infty)} - \frac{1}{\tau(0)} \right) [1 - \exp(-R_{\text{def}} t)] = \\ &= k \left[1 - \exp\left(-t/\tau_{\text{def}} \right) \right] \,. \end{aligned} \tag{3.4}$$

The resulting SRC degradation rate R_{SRC} has been observed as light-intensity independent above 1 mWcm^{-2}.[144] The degradation rate R_{SRC} was first thought to increase with [B$_\text{s}$]^2,[152] until Macdonald et al.[153] observed a degradation rate proportionality to p_0^2 in both B-Si and phosphorus-compensated B-Si.

3.1.2 Activation energy

The activation energy E_{def} of the LID defect formation can be obtained by measuring the degradation rate R_{def} over a temperature range and fitting the result with

$$R_{\text{def}}(T) = \kappa_0 \exp\left(-E_{\text{def}}/k_B T \right) \,. \tag{3.5}$$

In clean Cz-Si, fast degradation (FRC) has been associated with the formation activation energy of 0.23 ± 0.02 eV and slow degradation (SRC) with 0.475 ± 0.035 eV.[154] The activation energies have shown no dependency on the wafer boron or oxygen concentrations, but the pre-exponential κ_0 has been found to increase with increasing boron doping.[154]

Full dissociation of the FRC and the SRC defect has been observed after 10-min annealing at 200°C in the dark.[15] The SRC defect has recovered

with the activation energy of 1.32 ± 0.05 eV, while FRC recovery has been observed as a two stage process with the activation energies of 0.32 ± 0.01 eV and 1.36 ± 0.08 eV.[154] However, subsequent illumination has shown to reform the degradation,[15] prompting the FRC and the SRC defect to be classified as metastable.[144]

3.1.3 Metastable defect

The metastable SRC defect has been observed to form a deep energy level at $E_\mathrm{C}-0.41$ eV[155] with the carrier-capture cross-section ratio of σ_n/σ_p=10± 1.[155,156] The FRC level has been estimated as $E_\mathrm{C}-(0.35\text{-}0.85)$ eV with $\sigma_n/\sigma_p=100\pm10$.[154] The composition of both defects have been examined through the saturated normalized defect density $N_\mathrm{t}^*(\infty)$, which is defined in Eq. 3.4 and reflects the light-induced defect density. Some studies in p-Si[144,154] and gallium co-doped p-Si[157,158] have found $N_\mathrm{t}^*(\infty)$ to be proportional to [B_s], while others have observed a net doping $p_0=N_A-N_D$ dependency in p-Si compensated with phosphorus[153,159,160] or thermal donors.[161] Although some studies have reported no relation between $N_\mathrm{t}^*(\infty)$ and boron or oxygen,[146] results indicating $N_\mathrm{t}^*(\infty)$ dependency on both [B_s] and $[O_i]^2$ have attributed the degradation to the formation of a boron-oxygen complex.[144,154]

As experimental data have accumulated, the proposed BO complex has changed from B_iO_i[138] to B_sO_{2i},[144] and to a combination of B_sO_{2i} (FRC) and B_iO_{2i} (SRC).[139,162] After eliminating the involvement of oxygen dimers (O_{2i}),[163] Voronkov and Falster[137] have proposed a X_iB_sO complex, where X is a fast-diffusing interstitial impurity with a +1 charge that exists mostly in a precipitated state such as boron. In this model, B_iB_sO is presumed to form at low temperatures through B_iO dissociation and consequent B_i reaction with B_sO. Thus, the frozen-in concentration of B_iB_sO is thought to be proportional to both p_0 and $[O]^2$, although the complex only contains one oxygen atom.

Since LID has recently been observed in aluminum-doped Cz-Si in addition to indium-doped Cz-Si and FZ-Si,[17,18] metastable defect formation has shown not to require boron or oxygen. Therefore, Möller and Lauer[17,18] have proposed an acceptor and silicon self-interstitial complex as the metastable light-induced defect. The low initial lifetime in Al-doped Cz-Si has been attributed to the formation of an aluminum-oxygen complex.[164–166]

3.1.4 Mitigating degradation

Minimizing boron and oxygen

Boron-oxygen LID has traditionally been mitigated by minimizing the concentration of boron or oxygen in the silicon bulk.[16] Reducing the oxygen concentration below 1 ppm is effective, as no LID has been measured in clean boron-doped FZ-Si (Fig. 3.1) or 5.2 Ω-cm magnetic Czochralski (MCz) Si with 0.99 ppm of oxygen.[16,167] However, low-oxygen MCz-Si and FZ-Si ingot growth is known to be more expensive than conventional Cz-Si.

Replacing the boron doping with gallium has also proven effective, as no LID has been measured in gallium-doped p-type Cz-Si, regardless of oxygen concentration.[138,167] However, the low segregation coefficient of gallium has made the growth of uniform-resistivity Ga-doped Cz-Si ingots very challenging.[168] LID can additionally be mitigated by switching the solar cell bulk from p-Si to n-Si, since no degradation has been measured in clean phosphorus-doped Cz-Si[138] or phosphorus-doped FZ-Si with the increased oxygen level of 8.4 ppm.[169]

Regeneration

In Cz-Si with high boron and oxygen concentrations, Herguth et al.[170] have deactivated the metastable defects completely by the means of simultaneous illumination and annealing at $65-210$°C,[170–172] known as regeneration. During regeneration, the metastable defect is formed during the first few minutes of simultaneous illumination and annealing, but then dissociated with the activation energy of $0.61-0.71$ eV.[170–172] The regeneration rate has been shown to depend on both the temperature and the illumination intensity.[171] After defect dissociation, further illumination has caused no severe defect formation, but some lifetime instability has still been observed.[172] The deactivation rate has been observed to be inversely proportional to the boron concentration[173] and directly proportional to the oxygen concentration.[174] The deactivation process has also been found to be related to concentration of hydrogen that diffuses from the hydrogen-rich solar cell anti-reflection coating of silicon nitride into the silicon bulk during regeneration.[175,176] Approximately 4 h of dark annealing at 200°C has been shown to reverse the deactivation process, causing full metastable defect formation during subsequent illumination.[170]

3.1.5 Multicrystalline silicon

In addition to Cz-Si, LID has been measured in different types of multicrystalline silicon.[14,19–21,136,177,178] In some mc-Si materials, a smaller LID effect has been observed than in similar resistivity Cz-Si, which has been regarded as a result of a lower oxygen[136,178] or a higher carbon[179,180] concentration. Less degradation is also thought to occur in mc-Si simply due to a lower initial minority carrier recombination lifetime[177–179] caused by high levels of transition metals and high densities of extended defects, such as stacking faults, grain boundaries, and dislocations. Macdonald et al.[178] have observed a super-linear defect density dependence on $[O_i]$ at low oxygen concentrations, which changes into a near-quadratic dependence at high oxygen concentrations. As the measured degradation varied greatly between grains, interstitial oxygen has been suggested not to be directly involved in defect formation.[178]

In other mc-Si materials, stronger degradation has been measured than predicted by BO-LID theory.[14,19–21] Particularly mc-Si grown from upgraded metallurgical grade (UMG) silicon feedstock has shown relative efficiency losses of more than 10%.[19] Since using UMG-Si feedstock is known to increase the metal contamination concentration in the mc-Si ingot,[181] the stronger LID might be linked to copper-related degradation.

3.2 Copper-related degradation

In 1998, Henley et al.[8] and Tarasov et al.[182] observed light-induced degradation of the minority carrier diffusion length in $9-20$ Ω-cm p-type Cz-Si contaminated with copper concentrations lower than the doping level. Henley's samples had been oxidized to prevent copper out-diffusion,[42] and copper-related LID (Cu-LID) was separated from iron-related recombination by cyclic[182] and long-term[8] illumination. Later, Cu-LID was also observed in $0.5-2$ Ω-cm p-type FZ-Si[9,140] and >5 kΩ-cm n-type FZ-Si,[140] confirming that copper can cause LID even without boron and oxygen.

3.2.1 Degradation rate and defect density

Figure 3.2 depicts copper-related lifetime degradation measured with µ-PCD in homogeneous high-resistivity B-doped Cz-Si and with a low bulk micro-defect (BMD) density. Since Cu-LID displays single exponential de-

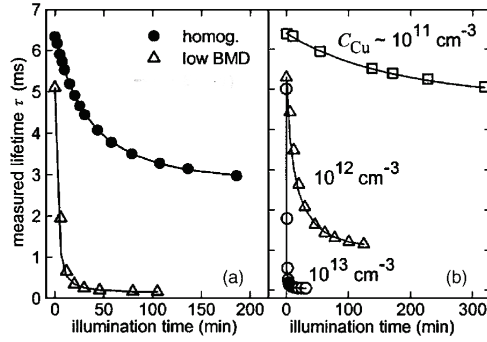

Figure 3.2. Effective minority-carrier recombination lifetime as a function of illumination time in a) homogeneous (oxygen precipitates $<10^6$ cm^{-3}) and low bulk micro-defect density (oxygen precipitates 5×10^8 cm^{-3}) Cz-Si with the copper concentration of 5×10^{12} cm^{-3}, and b) low bulk micro-defect density Cz-Si with different copper concentrations.[183] (Reprinted with permission from H. Väinölä, E. Saarnilehto, M. Yli-Koski, A. Haarahiltunen, J. Sinkkonen, G. Berenyi, and T. Pavelka, *Appl. Phys. Lett.* **87**, 032109 (2005). Copyright 2005, AIP Publishing LLC.)

cay in all samples, the degradation rates have been obtained by fitting the lifetime decay with the same degradation model as BO-LID in Eq. 3.4. The degradation rate of Cu-LID has been found to increase with increasing illumination intensity[9,10] and increasing copper concentration,[140,183] as shown in Fig. 3.2.b. The presence of oxygen precipitates[184,185] has also been observed to increase the degradation rate, as displayed in Fig. 3.2.a.

The saturated normalized defect density $N_t^*(\infty)$ has been found to increase with increasing BMD density[184,185] and be proportional to the interstitial copper concentration.[183] Therefore, $N_t^*(\infty)$ has been used to estimate the initial interstitial copper concentration C_{Cu} in defect-free silicon by[183]

$$C_{Cu} = \sqrt{\frac{N_t^*(\infty)}{(4.0 \pm 0.5) \times 10^{-24}}}\ (\mathrm{cm}^{-3})\,, \tag{3.6}$$

and in silicon with high BMD density by[183]

$$C_{Cu} = \frac{N_t^*(\infty)}{(3.0 \pm 0.2) \times 10^{-8}}\ (\mathrm{cm}^{-3})\,, \tag{3.7}$$

when $N_t^*(\infty)$ is obtained by µ-PCD lifetime measurements. The copper detection limit has been determined as some 5×10^{12} cm^{-3} in defect-free Si and below 10^{10} cm^{-3} in high BMD density material such as mc-Si.[183] A higher BMD density has been shown to render Cz-Si more sensitive to lower copper concentrations compared to FZ-Si.[140] Cu-LID kinetics are further examined in this work, and the main results are presented in Sec. 4.3 and 4.4.

3.2.2 Copper-related defect

The light-induced copper-related defect has been found to fully dissociate during a 1 min Rapid Thermal Anneal at 900°C.[11] As 900°C is high enough to dissolve a wide range of copper-related defects,[4,186–188] the dissociation temperature only eliminates defects with low dissociation temperatures such as pure copper complexes, discussed in Sec. 2.1.2. Although the defect responsible for Cu-LID is yet to be identified, Cu-LID has been proposed to occur due to substitutional copper release, copper precipitation, or surface passivation degradation by defect formation in the Si/SiO_2 interface. The origin of Cu-LID is further investigated in this dissertation, and the results are summarized in Sec. 4.2.

Substitutional copper

Illumination has been shown to decrease the DLTS peak of the pure copper complex (E_V+0.07 eV) and consequently form new peaks deeper in the silicon bandgap.[73,182] Since the copper complex was thought to be a Cu_sCu_i pair,[64,65] Henley et al.[8] and Ramappa[9] have suggested that illumination dissociates copper complexes, increasing the concentration of recombination-active Cu_s. Although the copper complex has since been identified as a complex of four copper atoms in Sec. 2.1.2,[66,67] the complex is still very likely to contain substitutional copper.[62,68,69]

As discussed in Sec. 2.1.4, copper complex dissociation was also suggested as the cause for lifetime degradation during dark annealing above 100°C.[9,91] Thus, Ramappa[9] has proposed that substitutional copper is responsible for both light-induced degradation and low-temperature degradation. Cu-LID has even been proposed to form with the same 0.419 eV[9] activation energy as in low-temperature lifetime degradation. However, this activation energy is unlikely to represent copper complex dissociation, as complex dissociation has only been observed above 150°C.[73]

Copper precipitates

High-intensity illumination is known to split the Fermi level into electron and hole quasi-Fermi levels E_{Fn} and E_{Fp}, respectively.[150] When E_{Fn} exceeds $E_C-0.2$ eV, Yli-Koski[185] and Väinölä et al.[10] have observed a clear increase in the copper-related degradation rate, and Belayachi et al.[11] have noticed a significant trapping of Cu_i^+ in the bulk. Since $E_C-0.2$ eV is known from Sec. 2.1.3 as the neutrality level of copper precipitates,[40] above which $Cu_3Si^{0/-}$ starts to attract Cu_i^+,[58] Cu-LID has been suggested to originate from copper precipitation.[10] Copper precipitation is proposed

to mainly occur as a result of a Cu_3Si charge change, but an illumination-induced change in the Cu_i^+ charge state cannot be ruled out.

Assuming that the degradation rate is proportional to the precipitation rate and the precipitate size is fixed, the light-induced precipitate radius r and density n could be obtained from the degradation time constant τ_{def} in Eq. 3.4 by[189]

$$\tau_{def} = \left(4\pi n r D_{Cu,eff}\right)^{-1} , \tag{3.8}$$

where $D_{Cu,eff}$ is the effective copper diffusivity in Eq. 2.2 at the illumination temperature.

Interface defects

Although a positive surface oxide has been observed to prevent copper out-diffusion,[42] as displayed in Fig. 3.3.a and discussed in Sec. 2.1.2, Boehringer et al.[12] have measured a large interface defect density D_{it} increase in oxidized $5.5-10.5$ Ω-cm p-type Cz-Si during 2.5 Wcm^{-2} illumination. The significant D_{it} increase was accompanied by a total positive surface charge increase. Therefore, 2.5 Wcm^{-2} illumination has been proposed to be intense enough to reduce the surface potential ϕ_s to near zero,[39] allowing Cu_i to diffuse towards the wafer surface and increase the Si/SiO_2 interface defect density, as suggested in Fig. 3.3.b.

Based on the D_{it} increase, Boehringer et al.[12] have concluded that the measured lifetime degradation is caused solely by a surface recombination

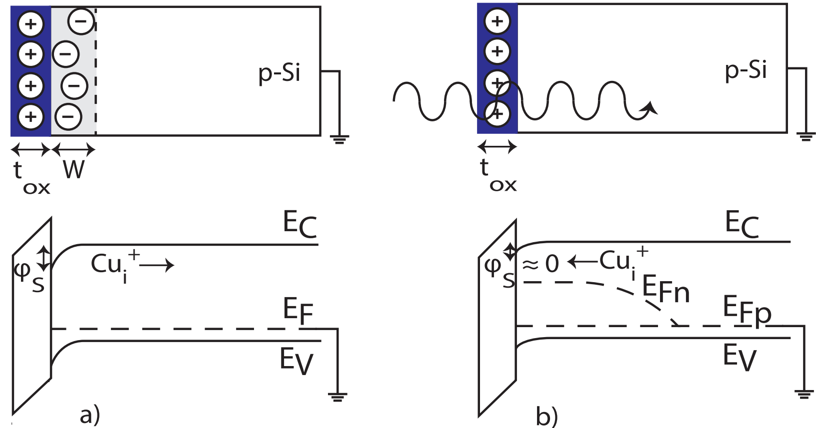

Figure 3.3. Cross-section and band diagram of p-type Si with a surface oxide of t_{ox} a) in the dark, and b) during illumination. The positive oxide charge depletes the width W of majority carriers and induces a surface potential ϕ_s. Intense illumination collapses the depletion area due to high excess carrier densities, splitting the Fermi level into the electron and the hole quasi-Fermi levels E_{Fn} and E_{Fp}, respectively. Consequently, the surface potential is reduced to near zero, which might cause Cu_i^+ diffusion towards the Si/SiO_2 interface.

increase. However, Belayachi et al.[11] have shown that interstitial copper begins to trap in the bulk even in bare p-Si, when the light intensity exceeds some 0.5 Wcm^{-2}. Since only 10 min of 5 Wcm^{-2} illumination has been sufficient to completely trap copper in the bulk of a bare p-Si wafer,[11] Cu-LID is less likely to have been caused only by a surface recombination increase at 2.5 Wcm^{-2} in oxidized Si. In order to further reduce the risk of copper diffusion towards the Si/SiO_2 interface during illumination, Yli-Koski et al.[190] and Väinölä et al.[10] have proposed applying additional positive corona charge to the surface oxide.

3.2.3 Mitigating copper

In order to minimize copper-related recombination in the silicon bulk, several methods have been developed to decrease the impurity concentration. These methods include copper out-diffusion, phosphorus diffusion gettering (PDG), and p/p^+ gettering through aluminum or heavy boron doping. This dissertation examines the effect of copper out-diffusion and PDG on copper-related LID. The main results are reported in Sec. 4.6.

Out-diffusion

As discussed in Sec. 2.1.2, interstitial copper is known to diffuse to the surface of a bare p-Si wafer even at RT.[40–42] Copper out-diffusion has been shown to accelerate during annealing[42,191] at $100-400$°C or continuous deposition of negative surface charges[192] such as corona charges (CO_3^-). During hot-plate annealing, 80% of the copper concentration has been found to diffuse to the cooler non-contact sample surface,[42] while negative charging has resulted in the majority of Cu_i^+ diffusing towards the negatively charged bare surface.[192]

In oxidized p-Si, negative surface charging has also been suggested to reduce the bulk copper concentration, as a negative corona density of -1 µCcm^{-2} has been shown to prevent Cu-LID in high-resistivity Cz-Si with small oxygen precipitates.[10,185,190] Negative corona charges have been proposed to attract Cu_i^+ towards the Si/SiO_2 interface, but without forming copper-related interface defects, since redeposition of positive corona charges (H_3O^+) has been shown to cause Cu-LID after copper diffusion back into the wafer bulk.[190] However, the redeposition of positive corona charges has only been tested on negatively charged sample unexposed to illumination.[190] Chemical analysis is also yet to confirm the location of copper in oxidized Si with positive and negative surface charge densities.

Gettering

Phosphorus, boron, and aluminum gettering are well-known segregation gettering methods for decreasing the bulk copper concentration. Segregation gettering at high temperatures relies on copper diffusion into a P-doped layer, heavily B-doped layer, or an Al-Si liquid due to a higher copper solubility.[193,194] In silicon solar cell manufacturing, phosphorus diffusion gettering (PDG) occurs during phosphorus in-diffusion (*e.g.,* emitter formation), boron gettering occurs during boron in-diffusion (*e.g.,* back-surface field formation), and aluminum gettering takes place during contact firing.

A PDG step around 900°C exceeding one hour has been confirmed as a very efficient method to remove copper from the silicon bulk.[4,186–188] PDG gettering has been modeled by the distribution of Cu_i, Cu_s and CuP pairs,[194] but the experimental segregation coefficient is yet to be determined, as several experimental studies have reported a copper concentration below detection limit after PDG.[4,186] Aluminum gettering for 2 h at 800°C has resulted in a segregation coefficient of at least $(1-2)\times10^3$, estimating a 90% copper concentration decrease in a 240-µm-thick wafer with a 1 µm aluminum layer.[195]

4. Results and Discussion

This chapter summarizes the main results on copper-related LID and nickel diffusivity in Publications I-VI. Cu-LID formation kinetics are emphasized in order to ascertain the origin of Cu-LID and to help distinguish between Cu-LID and BO-LID.

4.1 Materials affected by copper-related LID

Although BO-LID has been shown not to affect silicon with low boron and oxygen concentrations[16,167] in Sec. 3.1.4, Cu-LID has been observed in both low-resistivity B-doped FZ-Si[9,140] and very high-resistivity P-doped FZ-Si.[140] Since Cu-LID can form in FZ-Si without BO-LID, other silicon materials may also be prone to Cu-LID.

In order to determine the extent of Cu-LID in silicon, different Cz-Si and mc-Si materials were subjected to intentional copper contamination. Publications II, III, and IV show Cu-LID in low-resistivity Cz-Si and confirm previous observations of Cu-LID in high-resistivity Cz-Si.[8,140,182] Publication V detects Cu-LID in industrial low-resistivity mc-Si, and Publication I reveals Cu-LID in low- and high-resistivity Ga-doped Cz-Si. Table 4.1 lists all materials known to suffer from Cu-LID and indicates whether BO-LID also occurs.

Although Cu-LID occurs in both B-doped Cz-Si and FZ-Si, Cz-Si has been observed as more sensitive to low copper concentrations than FZ-Si.[140] In Publication I, B-doped Cz-Si additionally appears to be more sensitive to copper than Ga-doped Cz-Si. As the B-Si and the Ga-Si wafer thicknesses differed, the higher copper sensitivity of B-Si still needs to be confirmed by copper concentration measurements. Nevertheless, the effect of doping concentration on Cu-LID is summarized in Sec. 4.3.

In Publication V, Cu-LID is not only detected in intentionally contami-

Table 4.1. Silicon materials affected by Cu-LID and possibly BO-LID.

Material	Doping	Resistivity (Ω-cm)	Cu-LID	BO-LID
FZ-Si	B	0.5−2	Yes[9,140]	No[140]
	P	>5000	Yes[140]	No[140]
Cz-Si	B	2.7−3.9	Yes[II, III, IV]	Yes[II, III, IV]
	B	9−22	Yes[8,10,140,182,183]	Yes[140]
	B	18−24	Yes[II, IV]	Yes[IV]
	Ga	0.41	Yes[I]	No[I]
	Ga	10.1	Yes[I]	No[I]
mc-Si	B	1.3−2.0	Yes[V]	No[V]

nated mc-Si, but also in oxidized reference samples from the middle and the top of the ingot. Although high total copper concentrations are expected in the top part of the mc-Si brick,[3] all dissolved copper is assumed to precipitate heterogeneously after the high-temperature processing, due to the high density of extended defects with low precipitation barriers.[2,196] However, Publication V shows that copper concentrations of 10^{12} cm^{-3} can be kept as interstitials in low-resistivity p-type mc-Si after thermal oxidation at 900°C followed by air cooling.

4.2 Bulk versus surface LID

4.2.1 Surface passivation stability

Although BO-LID has previously been confirmed as a bulk recombination effect,[138] the surface passivation must be kept stable in LID studies, in order to accurately determine the saturated normalized defect density $N_t^*(\infty)$ with Eq. 3.2 and 3.3. In Publications I-V, most Cz-Si samples are passivated by a thermal oxide with a low interface defect density D_{it} of 3.6×10^{10} cm^{-2}eV^{-1}. Although dry oxidation provides excellent chemical surface passivation, the built-in positive charge density of 2.0×10^{11} cm^{-2} is not high enough to create good field passivation. Therefore, the field passivation of thermal oxide is improved by the deposition of external positive corona charge before illumination.

In Publication V, some samples were also passivated with aluminum

oxide (Al_2O_3) with a built-in negative surface charge of -7×10^{12} cm^{-2}.[197] Figure 4.1.a presents the effective lifetime in low-resistivity FZ-Si with Al_2O_3 and corona-charged thermal oxide during halogen illumination measured with QSSPC and during bias laser illumination measured with µ-PCD. Figure 4.1.b presents the temperature of a dummy wafer placed under the sample during halogen illumination, and the sample temperature near the illumination spot during bias laser illumination.

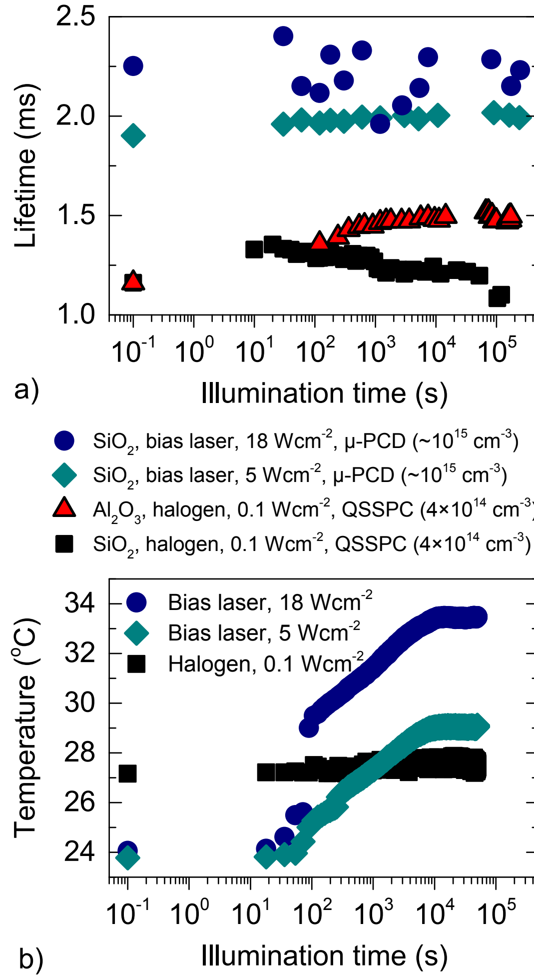

Figure 4.1. a) Effective lifetime in 1-5 Ω-cm B-doped FZ-Si with corona-charged (+0.26 µCcm^{-2}) thermal oxide during 0.1 Wcm^{-2} halogen illumination measured with QSSPC (Δn=4×10^{14} cm^{-3}), aluminum oxide during 0.1 Wcm^{-2} halogen illumination measured with QSSPC (Δn=4×10^{14} cm^{-3}), and corona-charged (+0.52 µCcm^{-2}) thermal oxide during 5 and 18 Wcm^{-2} bias laser illumination measured with µ-PCD (Δn~10^{15} cm^{-3}). b) Temperature of a dummy wafer placed under the sample during 0.1 Wcm^{-2} halogen illumination, and the sample temperature near the illumination spot during 5 and 18 Wcm^{-2} bias laser illumination.

Thermal oxide

In Fig. 4.1.a, the effective lifetime in corona-charged and thermally oxidized FZ-Si remains stable during 973.5-nm bias laser illumination regardless of the intensity, even though the sample temperature increases during illumination. As the passivation remains stable, the degradation observed during bias laser illumination in clean Cz-Si in Publication II reflects pure bulk BO-LID.

During halogen illumination, a fan was positioned less than 1 m from the sample to achieve an air flow that stabilizes the temperature, without reducing the front surface corona charge density. In corona-charged oxidized FZ-Si in Fig. 4.1.a, halogen illumination causes first a lifetime increase, followed by a slow decrease back to its initial value. The initial lifetime increase could be caused by FeB pair splitting due to unintentional iron contamination, but the slow decrease might be a result of increased surface recombination.

As the surface recombination is influenced by the chemical surface passivation, Figure 4.2 presents the Si/SiO_2 interface defect density D_{it} in clean and copper-contaminated B-doped Cz-Si before and after halogen illumination, measured in Publication IV. With only thermal oxide (0.2×10^{12} cm^{-2}), a clear D_{it} increase is observed in the clean reference sample after illumination, while the D_{it} hardly changes during illumination of the corona-charged (1.8×10^{12} cm^{-2}) reference. Therefore, the surface passivation of corona-charged clean samples appears to be relatively stable during halogen illumination in Publications III and IV. The D_{it} increase

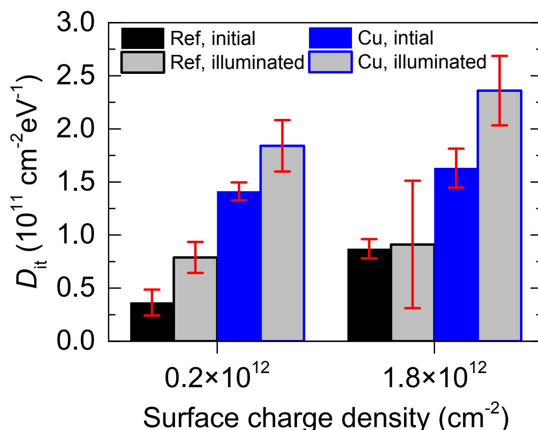

Figure 4.2. Interface defect density D_{it} as a function of surface charge density in clean (Ref.) and 1-ppm copper-contaminated (Cu) oxidized low-resistivity B-doped Cz-Si measured before (initial) and after (illuminated) 0.1 Wcm^{-2} halogen illumination.

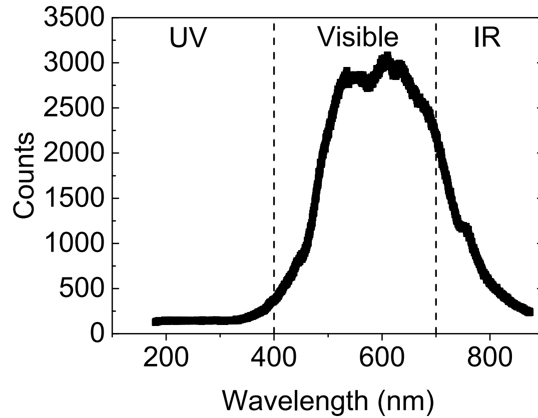

Figure 4.3. Halogen lamp spectrum measured with an OceanOptics UV-Visible spectrometer.

measured in the oxidized sample without corona (0.2×10^{12} cm^{-2}) could be caused by unintentional copper-related defects or ultraviolet (UV) degradation of the thermal oxide layer,[198,199] as UV wavelengths are present in the halogen lamp spectrum, as seen in Fig. 4.3.

Aluminum oxide

In Fig. 4.1.a, halogen illumination causes a slow lifetime increase in Al_2O_3-passivated FZ-Si. As the lifetime decreases back to 1338 µs after five days of storage in the dark, the measured lifetime increase could be a result of a light-induced Al_2O_3 charge-density increase.[141,142] Since aluminum oxide appears to be unstable during illumination, Al_2O_3 passivation might underestimate the extent of bulk degradation at high effective lifetimes. Nevertheless, the low lifetimes measured in mc-Si in Publications III are clearly dominated by bulk recombination, decreasing the impact of Al_2O_3 passivation improvement during illumination.

4.2.2 Copper-related LID

Although Cu-LID has previously been observed to correlate with an interstitial copper concentration decrease[11] and a minority carrier recombination lifetime/diffusion length decrease,[8–10,140,182–185,190] it is yet to be determined whether Cu-LID is caused by bulk or surface recombination. Boehringer et al.[12] have de facto measured a significant increase in the Si/SiO_2 interface defect density D_{it} during illumination, associating Cu-LID solely with surface passivation degradation, as described in Sec. 3.2.2. In order to identify the recombination effect caused by Cu-LID, two experiments were devised in Publications III and IV.

Figure 4.2 presents the interface defect density D_{it} in clean and copper-contaminated B-doped Cz-Si before and after halogen illumination measured in Publication IV. Although a D_{it} increase of 7×10^{10} $cm^{-2}eV^{-1}$ is observed in the contaminated samples during illumination, the increase is clearly smaller than $\Delta D_{it}\approx5\times10^{11}$ $cm^{-2}eV^{-1}$, which was measured by Boehringer et al.[12] in oxidized Cz-Si with a similar copper concentration.

If the D_{it} increase were caused by copper-related interface defect formation during illumination, Cu-LID would be caused by either a pure surface recombination increase or a combination of surface and bulk recombination. In the case of pure surface recombination, removing the degraded Si/SiO_2 interface would completely remove the Cu-LID effect. Correspondingly, if Cu-LID were a combination of surface and bulk recombination, removing the degraded interface would result in partial recovery of Cu-LID. However, after a silicon surface etch and subsequent aluminum oxide (Al_2O_3) deposition, the degraded lifetime shows no improvement in Publication III, even though Al_2O_3 provides better surface passivation than corona-charged thermal oxide.[200,201] Therefore, Cu-LID is determined to be dominated by bulk recombination.

4.3 Impact of doping on copper-related LID

Publications I and IV investigate Cu-LID as a function of doping concentration in Cz-Si. Figure 4.4 presents as summary the effective lifetime in oxidized copper-contaminated B-Si and Ga-Si during halogen and bias laser illumination, respectively. Although Ga-doped Cz-Si is not affected by BO-LID, intentional copper contamination causes Cu-LID formation. The degradation time constants in Table 4.2 are obtained by fitting the lifetime with the single exponential decay of Eq. 3.4.

B-doped Cz-Si shows faster degradation than Ga-Si, even though the degradation is performed at a lower light intensity. In low-resistivity B-Si, Figure 4.4.a reveals fast initial degradation, a slower second degradation, followed by a third very slow degradation. The first fast initial degradation is fitted by Eq. 3.4, while the slower degradation reactions are fitted with the double exponential

$$N_t^*(t) = a\left[1-\exp(-t/\tau_{def2})\right] + b\left[1-\exp(-t/\tau_{def3})\right] , \qquad (4.1)$$

where τ_{def2} is the degradation time constant of the second slow degradation and τ_{def3} is the degradation time constant of the very slow final

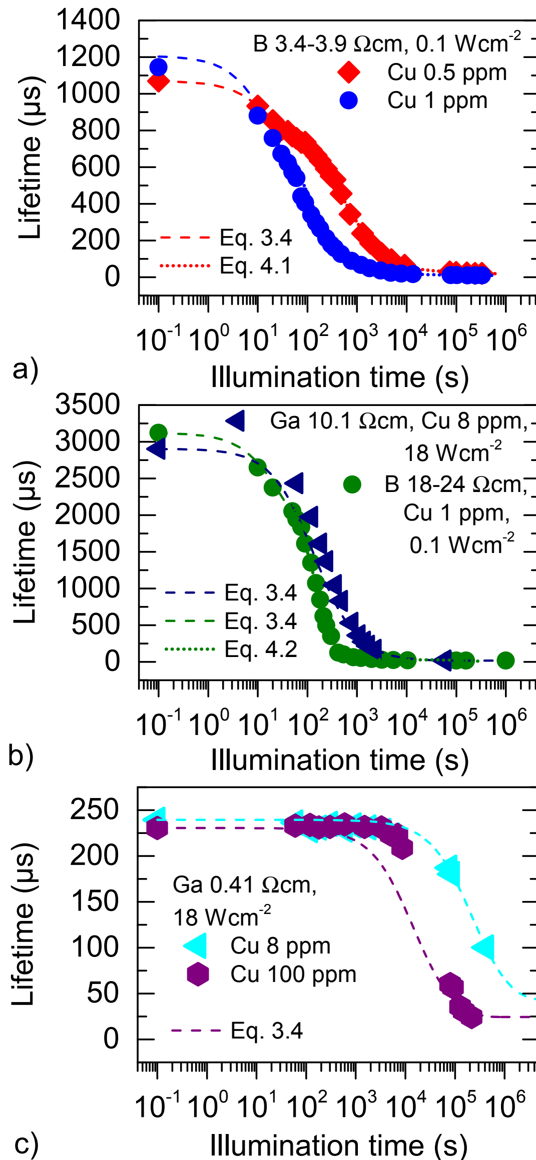

Figure 4.4. Effective lifetime as a function of illumination time in a) low-resistivity B-doped Cz-Si with Cu 0.5 and 1 ppm, b) high-resistivity B-doped Cz-Si with Cu 1 ppm and high-resistivity Ga-doped Cz-Si with Cu 8 ppm, and c) low-resistivity Ga-doped Cz-Si with Cu 8 and 100 ppm. The B-doped samples were illuminated with a 0.1 Wcm^{-2} halogen lamp and the effective lifetime was measured with QSSPC (Δn=4×10^{14} cm^{-3}). High-intensity bias laser illumination was employed in Ga-Si and the effective lifetime was measured with µ-PCD (Δn~10^{15} cm^{-3}).

Table 4.2. Copper contamination solution concentration and degradation time constants τ_{def} in B-doped and Ga-doped Cz-Si in Fig. 4.4.

Cz-Si	Cu solution (ppm)	$\tau_{\text{def}} = 1/R_{\text{def}}$ (s)
3.4-3.9 Ω-cm B-Si	0.5	27, 10570 & 161400
	1	55, 3980 & 66050
18-24 Ω-cm B-Si	1	56, 133 & 230570
0.41 Ω-cm Ga-Si	8	222600
	100	129300
10.1 Ω-cm Ga-Si	8	22610

degradation.

High-resistivity B-doped Cz-Si also shows fast initial degradation, a slower second degradation, and a third very slow degradation in Fig. 4.4.b. The first fast initial degradation is fitted by Eq. 3.4, but the slower degradation reactions are faster compared to low-resistivity B-doped Cz-Si and can be fitted with the double exponential

$$\tau_{\text{eff}}(t) = c\exp(-t/\tau_{\text{def4}}) + d\exp(-t/\tau_{\text{def5}})\,, \tag{4.2}$$

where τ_{def4} is the degradation time constant of the second slow degradation and τ_{def5} is the degradation time constant of the very slow final degradation.

In all samples, degradation becomes faster with an increasing copper concentration, as previously observed in literature.[140,183] In both B-doped and Ga-doped Cz-Si, higher doping concentrations slow down the degradation rate. Slower degradation could be explained by the higher concentration of copper-acceptor pairs, which need to dissociate before Cu-LID formation can occur. The higher dissociation energy of CuGa (0.71 ± 0.02 eV)[26,32] compared to CuB (0.61 ± 0.02 eV)[26,32] could also explain the slower degradation observed in Ga-Si compared to B-Si, even though Ga-Si was illuminated at a higher intensity and a higher temperature (as seen in Fig. 4.1.b).

4.4 Temperature dependence of copper-related LID

Publication IV presents Cu-LID as a function of illumination temperature in B-doped Cz-Si. Increasing the temperature increases the degradation rate, as expected from previous BO-LID results.[154] Fitting Eq. 3.5 to the slow degradation rate $R_{\text{def2}}/R_{\text{def4}}$ results in the activation energy of

0.323±0.090 eV in 3.4-3.9 Ω-cm Cz-Si and 0.146±0.025 eV in 18-24 Ω-cm Cz-Si, respectively. The obtained activation energies of slow degradation are low compared to the BO-LID SRC activation energy of 0.475±0.035 eV.[154] The activation energies are also clearly dependent on the doping concentration, while the activation energy of BO-LID has been shown to be independent of the boron and the oxygen concentration.[154] Moreover, the activation energies are lower than the temperature-induced copper-defect activation energy of 0.419 eV, which Ramappa[9] suggested as the activation energy of Cu-LID in Sec. 3.2.2.

In the high-resistivity material, the measured activation energy is close to the intrinsic diffusion energy of 0.18±0.01 eV.[26] In B-doped Si, interstitial copper is known to form CuB pairs with the dissociation energy of 0.61±0.01 eV.[26,32] Increasing the temperature or decreasing the doping concentration reduces the concentration of CuB pairs, increasing the effective copper diffusivity until the intrinsic copper diffusivity is achieved. Illumination might also increase the pair dissociation rate, further increasing the effective diffusivity. Therefore, the activation energies obtained in Publication IV might reflect the diffusivity of copper instead of the formation energy of Cu-LID. This interpretation makes copper diffusion the limiting reaction in the formation of copper-related LID.

Diffusion-limited Cu-LID would explain the slow degradation observed in Ga-Si, since the dissociation energy of CuGa is higher than that of CuB.[26,32] A higher Cu-acceptor pair concentration would also explain the slower degradation rates observed in highly doped B-Si and Ga-Si in Fig. 4.4. However, diffusion-limited Cu-LID would result in the formation of a low density of copper-related defects, which is less likely to cause such a large lifetime decrease, as measured in Fig. 4.4.

The degradation rate of Cu-LID has previously been shown to increase with increasing illumination intensity.[9,10] Publication V also reports a degradation rate dependence on the bias laser illumination intensity in a good-grain area of B-doped mc-Si. However, Figure 4.1.c shows a 4°C difference in the sample temperature between 5 and 18 Wcm^{-2} bias laser illumination. Therefore, further data is needed to determine whether the degradation rate increase is caused by the illumination intensity or the sample temperature increase.

4.5 Low-temperature stability

4.5.1 Before illumination

Since BO-LID defects are known to fully dissociate at 200°C,[15] Publication IV investigates the effect of low-temperature annealing on copper-contaminated Cz-Si. Figure 4.5 depicts the effective lifetime as a function of annealing time at 210 ± 10°C in contaminated (0.5 and 1 ppm) high- and low-resistivity B-doped Cz-Si. Before illumination, a lifetime decrease is observed in high-resistivity B-doped Cz-Si after a 2 min anneal, while the low-resistivity sample exhibits a lifetime increase. This lifetime increase might be caused by the recovery of BO-LID formed during sample preparation. However, in the same material with a higher copper concentration (8 ppm), a lifetime decrease is measured after 10 min at 210°C in Publication III.

Annealing for 1000 min results in lifetime degradation in all copper-contaminated samples regardless of resistivity, which is in agreement with previous stability experiments[9,91] above 100°C, as discussed in Sec. 2.1.4. During annealing, the interface defect density increases only from 1.6×10^{11} to 1.9×10^{11} $cm^{-2}eV^{-1}$ in the 1-ppm-contaminated low-resistivity sample. Therefore, bulk-related recombination is determined to dominate during low-temperature annealing. Lifetime degradation after long-term annealing might be caused by copper precipitation, as Cu-Si system studies have shown η''-Cu_3Si formation at 200°C.[93–95] In conclusion, the life-

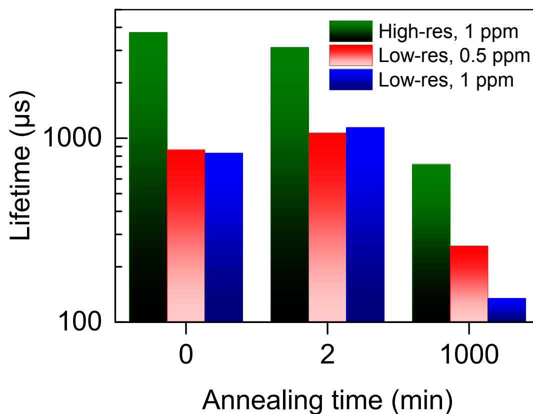

Figure 4.5. Effective lifetime as a function of annealing time at 210 ± 10°C in contaminated (0.5 and 1 ppm) high- and low-resistivity B-doped Cz-Si. (Reprinted with permission from J. Lindroos and H. Savin, *J. Appl. Phys.* **116**, 234901 (2014). Copyright 2014, AIP Publishing LLC.)

time behavior during low-temperature annealing before illumination is determined to depend on the boron concentration, copper concentration, and annealing time.

4.5.2 After illumination

Publications III and IV present the effective lifetime after Cu-LID formation and a dark anneal at 210 ± 10°C. Unlike the clean reference, illuminated low-and high-resistivity B-doped Cz-Si contaminated with copper solutions of 1 and 8 ppm do not recover during the 200°C anneal. Therefore, the light-induced copper-related defects at the aforementioned copper contamination levels are determined to be stable at 200°C. This result is in agreement with previous observations on Cu-LID defect dissociation requiring a temperature of 900°C.[11]

4.6 Mitigating copper-related LID

In p-Si, bulk copper contamination can be reduced by phosphorus diffusion gettering (PDG)[4,186–188] or copper out-diffusion,[10,41,42,185,190,192] as discussed in Sec. 3.2.3. Publications II-V investigate copper out-diffusion by negative surface charging and its impact on Cu-LID in Cz-Si and mc-Si. A negative surface charge is achieved by the deposition of negative corona charge or aluminum oxide with a built-in negative charge. Section 4.6.3 examines the effect of PDG on Cu-LID.

4.6.1 Negative corona charging

Chemical analysis

Since negative corona charge deposition has been shown to prevent Cu-LID in oxidized Cz-Si with oxygen precipitates,[10,185,190] negative surface charging has been proposed to attract Cu_i^+ towards the Si/SiO_2 interface, yet without increasing the surface recombination.[185,190] Although surface copper accumulation has been confirmed by chemical analysis in bare Si wafers,[192] copper accumulation and its effect on the surface passivation remains to be determined in oxidized p-Si.

Figure 4.6.a presents the total surface copper concentration measured with Total Reflection X-Ray Fluorescence (TXRF) as a function of surface corona charge density in oxidized low-resistivity B-doped magnetic Czochralski (MCz) Si, contaminated with copper solutions of 1, 8, and 16

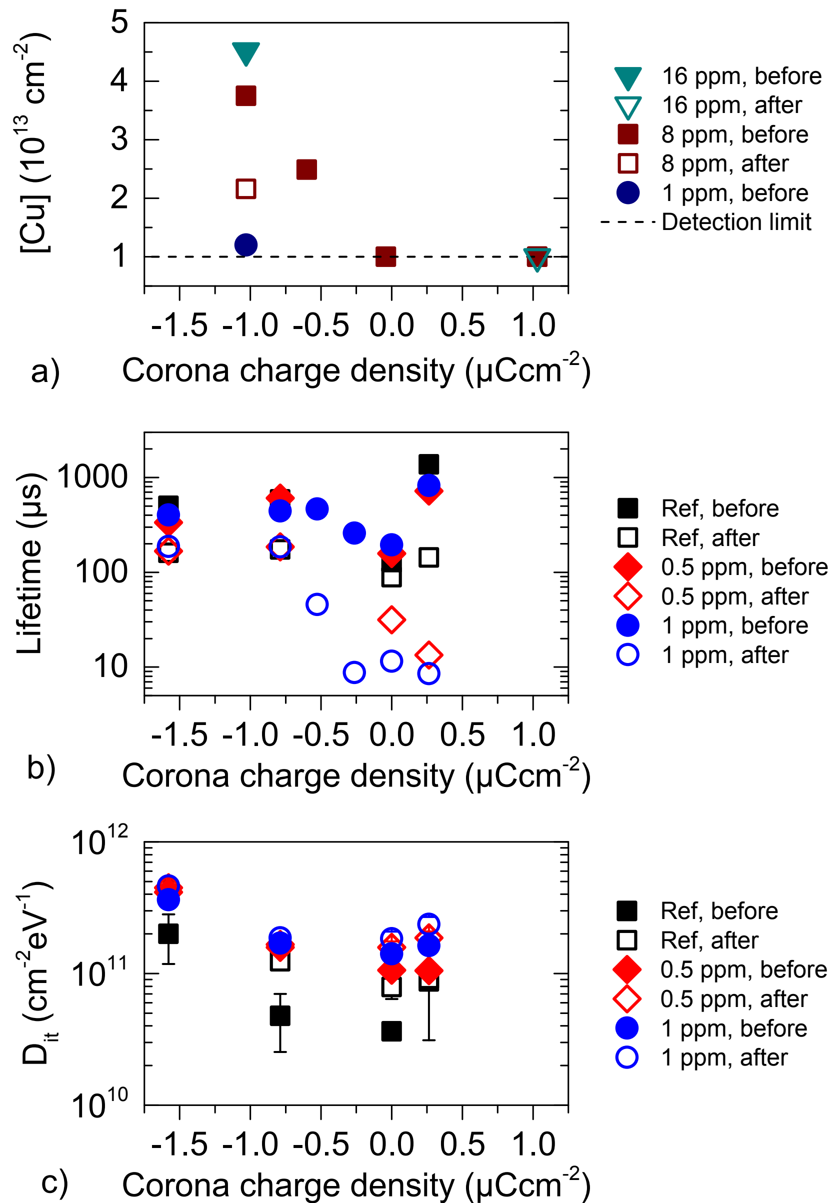

Figure 4.6. a) Near-surface copper concentration as a function of corona charge density in oxidized 400-μm, 2.4−3.6 Ω-cm B-doped MCz-Si contaminated with copper solutions of 1, 8, and 16 ppm before and after 0.1 Wcm^{-2} halogen illumination. b) Effective lifetime measured with QSSPC (Δn=4×10^{14} cm^{-3}) and b) interface defect density $D_{\rm it}$ as a function of surface corona charge density in clean (Ref) and contaminated (0.5 and 1 ppm) low-resistivity B-doped Cz-Si before and after 0.1 Wcm^{-2} halogen illumination.

ppm. With a positive corona charge density, the near-surface copper concentration is below the detection limit before and after illumination. However, negative corona charging of -0.6 µCcm^{-2} reveals copper accumulation near the Si/SiO_2 interface. The near-surface copper concentration appears to increase not only with an increasing negative corona charge density, but also with an increasing initial bulk copper concentration. Hence, the applied negative corona charge is shown to also accumulate copper near the sample surface of thermally oxidized Si.

Charge density

Figure 4.6.b depicts the effective lifetime and Fig. 4.6.c shows the interface defect density D_{it} as a function of corona charge density in clean and contaminated low-resistivity B-doped Cz-Si, before and after halogen illumination. With a positive corona charge, the clean sample shows BO-LID, and the contaminated samples reveal more severe Cu-LID. Adding negative corona charge results in a lower initial lifetime in both the clean and the contaminated samples. The lower initial lifetime is a result of majority carrier accumulation, which causes higher surface recombination compared to positive-charge-induced inversion, as shown in Fig. 4.7.

At the high negative charge density of -1.58 µCcm^{-2}, the lower initial lifetime is also clearly a result of a high Si/SiO_2 interface defect density in Fig. 4.6.b. Nevertheless, the negative-charge-induced surface recombination increase does not impact significantly the final degraded lifetime, as bulk recombination has been shown to dominate both BO-LID[144] and Cu-LID in Sec. 4.2. In fact, increasing the negative charge density results

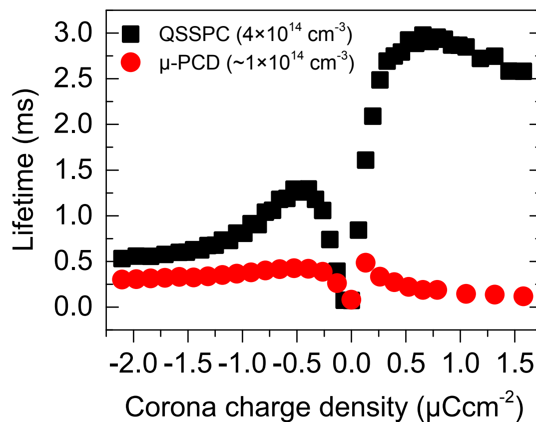

Figure 4.7. Effective lifetime as a function of surface corona charge density in oxidized low-resistivity FZ-Si measured with QSSPC (Δn=4×10^{14} cm^{-3}) and µ-PCD (Δn∼1×10^{14} cm^{-3}).

in less Cu-LID. In the contaminated samples, the final degraded lifetime increases with the increasing negative corona charge density, until the lifetime stabilizes around -0.78 μCcm^{-2}. Beyond this negative charge density, any additional copper collected towards the surface does not improve the final degraded lifetime, suggesting that the point of maximum Cu-LID removal has been reached in the sample.

Figure 4.8.a presents the effective lifetime as a function of illumination in clean and contaminated samples with -0.78 μCcm^{-2}. In both samples, the lifetime first increases slightly before decreasing during light-induced defect formation. The lifetime increase could be FeB pair dissociation, since it also appears in the contaminated samples without any added corona charge. As both the clean and the contaminated Cz-Si show similar lifetime behavior during illumination and saturate at nearly the

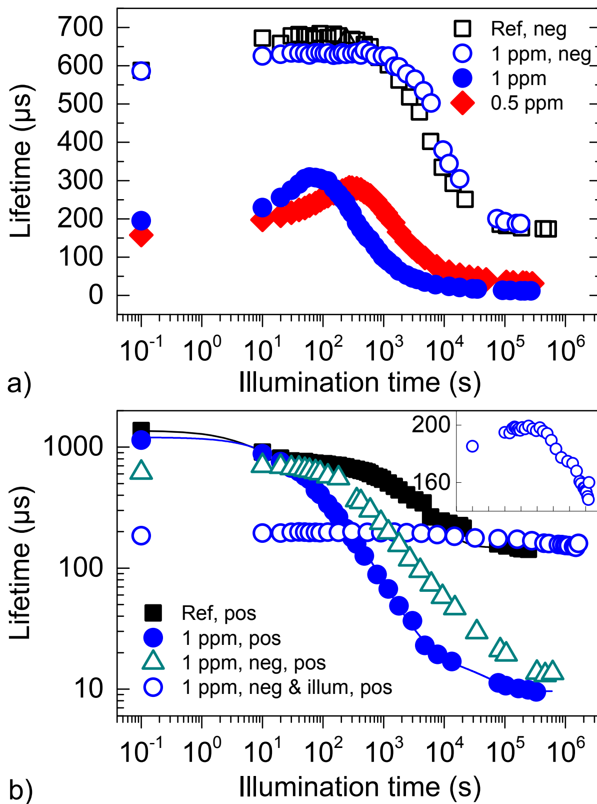

Figure 4.8. Effective lifetime as a function of illumination time in oxidized clean (Ref) and contaminated (0.5 and 1 ppm) low-resistivity Cz-Si with a) no corona and -0.78 μCcm^{-2} (neg), and b) cumulative corona charge of $+0.26$ μCcm^{-2} (pos). In b), the notation "neg" refers to a sample with previous negative charge and "neg & illum" to a sample previously illuminated with a negative charge. The inset shows the negatively charged sample illuminated in a) with redeposited positive charge (neg & illum, pos).

same lifetime value, accumulation of copper near the surface by a negative charge appears to completely prevent Cu-LID formation without affecting BO-LID. The negative charge density needed to prevent Cu-LID depends on the initial copper concentration, as shown in Publication II. Although Cu-LID in Publication II was fully prevented by -1.3 µCcm^{-2} in the 2-ppm samples and -1.58 µCcm^{-2} in the 8-ppm samples, respectively, all results were reported at -2.34 µCcm^{-2} for comparison. Cu-LID removal by negative corona charging is not only applicable in Cz-Si, as Publication V reports Cu-LID prevention in oxidized B-doped multicrystalline Si.

Illumination

Although the negative surface charge prevents Cu-LID formation, the redeposition of positive corona charge has resulted in Cu-LID,[190] presumably due to copper diffusion back into the bulk. Figure 4.8.b shows the effective lifetime as a function of illumination time in clean and contaminated Cz-Si with an initial positive charge. The figure also displays two contaminated samples with an initial negative charge, which has been compensated to $+0.26$ µCcm^{-2} by redepositing positive charge. In the sample with previous negative charging but no illumination (neg, pos), positive redeposition and illumination causes nearly as severe and fast Cu-LID as in the initially positively charged reference. This results indicates that nearly all copper has diffused back into the bulk after positive charge redeposition, which is agreement with Yli-Koski's previous observations.[190]

In the sample previously illuminated with a negative surface charge (neg & illum, pos), the initial lifetime is low after positive charge redeposition, since BO-LID defects have formed during the first illumination in Fig. 4.8.a. Nevertheless, after positive charge redeposition, the effective lifetime decreases only slightly during illumination, and the final lifetime remains at the saturation level of the BO-degraded reference sample. Hence, negative surface charging together with illumination appears to deactivate copper, preventing copper diffusion back into the bulk and Cu-LID formation.

Although Cu-LID deactivation could be a result of copper-related interface defect formation, hardly any D_{it} increase occurs during illumination in Fig. 4.6.c. Copper diffusion into the oxide is also less likely, as Fig. 4.6.a confirms that the majority of copper stays in the near-surface area after illumination. Even though copper is known to form many recombination-active defects in silicon as discussed in Sec. 2.1, illumination of surface-

accumulated copper might form a recombination-inactive defect that is stable at RT and insensitive to light, preventing copper diffusion back into the bulk. Further experiments are required to determine the state of copper after negative charging and illumination.

4.6.2 Aluminum oxide

In addition to corona charging, a negative surface charge can be achieved by Atomic Layer Deposition (ALD) of aluminum oxide with a built-in negative charge. In Publication V, Cu-LID is detected in B-doped mc-Si wafers from the middle and the top of the ingot. After Al_2O_3 deposition, no degradation is observed in either samples. Therefore, the Al_2O_3 charge density of 7×10^{12} cm^{-2} prevents the formation of Cu-LID in mc-Si with an estimated copper concentration of 5×10^{12} cm^{-2}. In Publication III, the 8-ppm-contaminated low-resistivity B-doped Cz-Si sample degraded already during aluminum oxide deposition or the post-anneal. Therefore, further investigation is required to determine under which conditions Al_2O_3 can be used to mitigate Cu-LID formation.

4.6.3 Phosphorus diffusion gettering

As phosphorus diffusion gettering (PDG) is an efficient method to reduce copper contamination in silicon, a PDG step will probably affect Cu-LID in silicon-based devices. Therefore, PDG is performed on top and middle B-doped mc-Si sister samples with previously observed Cu-LID in Publication V. First, a 1-µm thick gettering layer is formed with a phosphorus spin-on dopant during 60 min of P in-diffusion at 870°C in N_2 atmosphere, followed by a 4°C/min ramp to the unloading temperature of 800°C. This gettering treatment is more efficient compared to typical industrial P in-diffusions.[202] Next, the PDG glass is etched in 20% HF, and the P-doped layer is removed in HF:HNO_3:CH_3COOH. After standard cleanings, the samples are finally passivated with a thermal oxide (16 nm).

Figure 4.9 shows the lifetime in gettered top and middle mc-Si wafers with positive and negative corona charge before and after bias laser illumination. PDG improves the initial lifetime before illumination in all samples, due to the segregation of dissolved transition metals to the P-doped layer. During illumination, no degradation is observed in the oxidized middle sample, and the top wafer only displays very slight degradation. Therefore, the PDG treatment efficiently decreases the copper con-

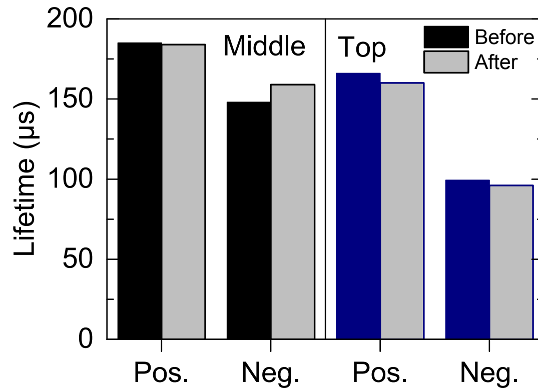

Figure 4.9. Effective lifetime in phosphorous diffusion gettered low-resistivity middle and top B-doped mc-Si samples passivated with positive and negative corona charge deposited on thermal oxide measured with µ-PCD before and after 18 Wcm^{-2} bias laser illumination.

centration to near the µ-PCD detection limit of Cu-LID in mc-Si. Since no degradation occurs after negative corona charging, copper is confirmed to be the sole cause of LID in the mc-Si material in Publication V.

4.7 Copper-related LID compared with boron-oxygen LID

Although B-doped Cz-Si has been determined to be the most sensitive Si material to both Cu-LID and BO-LID,[140] the two degradation effects have several distinguishing properties listed in Table 4.3. BO-LID is intensity independent,[144] while the Cu-LID rate has been shown to increase with increasing intensity,[9,10] even though the Cu-LID intensity-dependence still needs to be confirmed, as discussed in Sec. 4.4. BO-LID is known to fully recover at 200°C,[15] while no lifetime improvement is observed in Cz-Si with copper concentrations of 10^{14} cm^{-3} in Sec. 4.5. Finally, a negative surface charge is shown to prevent Cu-LID without affecting BO-LID in Sec. 4.6.1.

Although the above-mentioned properties help to distinguish between Cu-LID and BO-LID, they do not reveal the defect(s) formed during illumination. Negative surface charging may still leave a low copper concentration in the bulk, which might form BO-LID-type degradation during illumination. Cu-LID might not be intensity-dependent, and lower concentrations of Cu-LID defect may recover at 200°C. However, the Cu-LID activation energy dependency on the doping concentration indicates that Cu-LID is more likely to be a separate degradation effect from boron-

Table 4.3. Properties of boron-oxygen LID and copper-related LID.

Boron-oxygen LID	Copper-related LID
Sensitive to B and O[16]	Sensitive to B and O[140]
Fast and slow LID[143–146]	Fast, slow, very slow LID[I, II, IV, V]
Faster with increasing T[154]	Faster with increasing T[IV]
Requires both B and O[16] (or Al/In[18])	Requires neither B nor O[140]
Faster with high [B$_s$]/p_0[160,203]	Slower with high [B$_s$]/[Ga$_s$][II, IV]
Light-intensity independent[144]	Light-intensity dependent[9,10]
E_{def} independent of [B$_s$][154]	E_{def} dependent on [B$_s$][IV,*]
Recoverable at 200°C[15]	Not recoverable at 200°C[IV]
Unaffected by negative charge	Prevented by neg. charge[II, III, V]

$^*E_{def}$ might reflect effective copper diffusivity instead of Cu-LID.

oxygen LID.

4.8 Nickel diffusivity compared with copper diffusivity

In 1980, Bakhadyrkhanov et al.[98] obtained the most frequently cited nickel diffusivity with the activation energy of 0.47 eV, presented as Eq. 2.5 in Sec. 2.2.1. Since first principles calculations predict a much lower activation energy of 0.21 eV,[27,105] an accumulation experiment was designed to measure the diffusivity of nickel in Publication VI. The diffusion experiment relies on steady-state nickel diffusion from an infinite nickel silicide source through intrinsic silicon to an Al-Si gettering liquid. The nickel concentration in the Al-Si layer is determined as[101]

$$\begin{aligned} N_{\mathrm{Ni}}(T) &= J_{\mathrm{Ni}}(T)t = -D_{\mathrm{Ni}}(T)\frac{\Delta C_{\mathrm{Ni}}(T)}{\Delta x}t = \\ &= -D_{\mathrm{Ni}}(T)\left(\frac{0 - S_{\mathrm{Ni}}(T)}{d_{\mathrm{Si}}}\right)t = \frac{D_{\mathrm{Ni}}(T)S_{\mathrm{Ni}}(T)}{d_{\mathrm{Si}}}t\,, \end{aligned} \tag{4.3}$$

where $J_{\mathrm{Ni}}(T)$ is the nickel flux, t is the nickel collection time, $D_{\mathrm{Ni}}(T)$ is the nickel diffusivity, $C_{\mathrm{Ni}}(T)$ is the nickel concentration, $S_{\mathrm{Ni}}(T)$ is the nickel solubility in Eq. 2.6, and d_{Si} is the silicon thickness. In the experiment, the nickel diffusivity $D_{\mathrm{Ni}}(T)$ of

$$D_{\mathrm{Ni}}(T) = (1.69 \pm 0.74) \times 10^{-4}\exp(-0.15 \pm 0.04\,\mathrm{eV}/k_B T)\ \mathrm{cm^2 s^{-1}}\,. \tag{4.4}$$

is obtained in the temperature range of $665-885$°C.

Figure 4.10 compares the new nickel diffusivity result in Eq. 4.4 with the literature[98] nickel diffusivity in Eq. 2.5 and the copper diffusivity[26] in

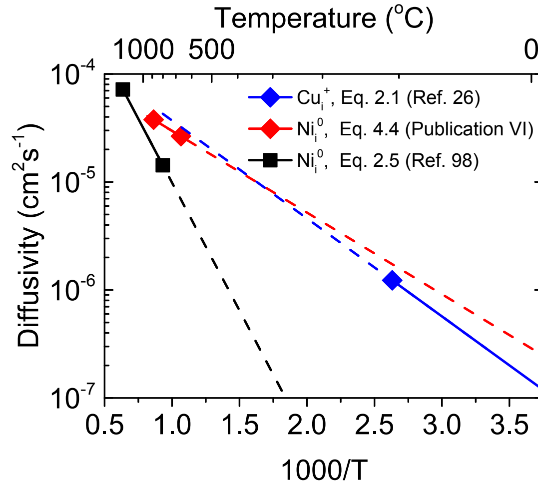

Figure 4.10. Measured diffusivity (lines) of copper and nickel in intrinsic silicon plotted (dashed lines) in the temperature range of $0-1300$°C.[26,98]

intrinsic silicon in Eq. 2.1. At 900°C, the new result gives the nickel diffusivity of $(3.83^{+4.35}_{-2.38})\times10^{-5}$ cm^{2}s^{-1}, and the literature diffusivity[98] results in a similar value of 1.91×10^{-5} cm^{2}s^{-1}. However, the two nickel diffusivity values diverge quickly with decreasing temperature, resulting in a estimated difference of four orders of magnitude at RT.

Even though the new nickel diffusivity result clearly differs from the literature diffusivity, the new activation energy of 0.15 ± 0.04 is closer to the calculated result of 0.21 eV.[27,105] The newly measured $D_{\mathrm{Ni}}(T)$ is also similar to the diffusivity of copper[26] over the whole temperature range of $27-800$°C. Therefore, Ni_i^0 is determined to be as fast a diffuser as Cu_i^+ in intrinsic silicon.

5. Conclusions

This dissertation examined the behavior of copper and nickel impurities in crystalline silicon. The activation energy of interstitial nickel diffusivity was measured as $0.15{\pm}0.04$ eV, which corresponds to the first principles calculations result of 0.21 eV, confirming nickel to be as fast a diffuser as interstitial copper.

Interstitial copper has been observed to form recombination-active defects during illumination, known as copper-related light-induced degradation (Cu-LID). In order to identify the extent of Cu-LID in silicon materials, the minority carrier lifetime was measured during illumination in intentionally copper-contaminated boron-doped Czochralski (Cz) silicon, gallium-doped Cz silicon, and boron-doped multicrystalline (mc) silicon. Cu-LID was determined to mainly cause bulk recombination, although some surface recombination increase was observed during halogen illumination. The small surface recombination increase may have been unrelated to copper, as a similar increase was measured in the clean reference wafers.

The degradation rate of Cu-LID was shown to depend on the dopant element and the doping concentration in p-type Cz-Si. Cu-LID formation became slower with increasing doping concentration, which was presumed to be caused by a higher concentration of CuB or CuGa pairs, which slow down copper diffusion. Faster Cu-LID formation in B-doped compared to Ga-doped Cz-Si was explained by the lower CuB dissociation energy of 0.61 eV[26,32] compared to CuGa with 0.71 eV.[26,32]

The activation energy of Cu-LID was measured as $0.323{\pm}0.090$ eV in low-resistivity B-Si and $0.146{\pm}0.025$ eV in high-resistivity B-Si, which clearly differed from the BO-LID activation energy of $0.493{\pm}0.054$ eV. As the Cu-LID experiments yielded low activation energies dependent on the boron concentration, questions were raised about the origin of the activation en-

ergy. The activation energy was proposed to reflect the effective copper diffusivity, making copper diffusion the limiting reaction in Cu-LID formation.

Cu-LID formation was decreased or prevented by two methods of bulk copper removal. After heavy phosphorus diffusion gettering, only slight Cu-LID was observed in the top of the B-doped mc-Si ingot with an estimated initial copper concentration of $5{\times}10^{12}$ cm^{-3}. After negative surface charging and illumination, Cu-LID was completely removed from contaminated B-doped Cz-Si. The negative surface charge was achieved through either aluminum oxide deposition or negative corona charging. TXRF analysis showed an increased accumulation of copper near the oxidized wafer surface as a function of an increasing negative surface charge density. The negative charge density required for full copper removal depended on the initial bulk copper concentration. After negative charging and illumination, copper remained recombination-inactive near the sample surface, preventing Cu-LID formation in the bulk.

Although illumination with a negative surface charge prevented Cu-LID, the method was shown not to affect BO-LID. Even though BO-LID is known to fully recover at 200°C,[15] no Cu-LID recovery was observed at estimated copper concentrations of 10^{14} cm^{-3}. Unlike BO-LID, the activation energy of Cu-LID was shown to increase with increasing doping concentration. Hence, BO-LID and Cu-LID were proposed as two different degradation reactions, forming separate recombination-active defects.

Even if Cu-LID and BO-LID were two different effects, they might still occur simultaneously in contamination-heavy silicon materials such as UMG-Si. Cu-LID might also appear together with BO-LID in better quality silicon through unintentional copper contamination during device processing. In order to better distinguish between Cu-LID and BO-LID, the Cu-LID defect energy level needs to be determined and the intensity dependency confirmed. To further understand the formation of Cu-LID, the degradation rate and defect density should be examined more widely as function of [O], [B], and p_0. To efficiently prevent Cu-LID formation, copper gettering by PDG should be optimized and further investigations should be performed on the application of negative surface charging in industrial silicon-based devices. Finally, regeneration of BO-LID should be optimized together with Cu-LID removal in order to fully prevent light-induced degradation in crystalline silicon.

References

[1] K. Graff, *Metal impurities in silicon-device fabrication*, (Springer, 2000), 2nd ed.

[2] A. A. Istratov, T. Buonassisi, R. J. McDonald, A. R. Smith, R. Schindler, J. A. Rand, J. P. Kalejs, and E. R. Weber, Metal content of multicrystalline silicon for solar cells and its impact on minority carrier diffusion length, *Journal of Applied Physics* **94**, 6552 (2003).

[3] D. Macdonald, A. Cuevas, A. Kinomura, Y. Nakano, and L. J. Geerligs, Transition-metal profiles in a multicrystalline silicon ingot, *Journal of Applied Physics* **97**, 033523 (2005).

[4] M. B. Shabani, T. Yamashita, and E. Morita, Metallic impurities in mono and multi-crystalline silicon and their gettering by phosphorus diffusion, *ECS Transactions* **16**, 179–193 (2008).

[5] M. Dhamrin, T. Saitoh, K. Kamisako, T. Mori, and N. Iwamoto, Recycling of silicon powder retrieved from diamond wire slicing kerf, in *Proceedings of the 25th European Photovoltaic Solar Energy Conference and Exhibition*, (Valencia, Spain, 2010), pp. 1600–1603.

[6] T. Hosoya, Y. Ozaki, and K. Hirata, Effects of wet cleaning on Si contaminated with heavy metals during Reactive Ion Etching, *Journal of the Electrochemical Society* **132**, 2436–2439 (1985).

[7] E. R. Weber, Transition metals in silicon, *Applied Physics A* **30**, 1–22 (1983).

[8] W. B. Henley, D. A. Ramappa, and L. Jastrezbski, Detection of copper contamination in silicon by surface photovoltage diffusion length measurements, *Applied Physics Letters* **74**, 278–280 (1999).

[9] D. A. Ramappa, Surface photovoltage analysis of phase transformation of copper in p-type silicon, *Applied Physics Letters* **76**, 3756–3758 (2000).

[10] H. Väinölä, M. Yli-Koski, A. Haarahiltunen, and J. Sinkkonen, Sensitive copper detection in p-type Cz silicon using µ-PCD, *Journal of the Electrochemical Society* **150**, G790–G794 (2003).

[11] A. Belayachi, T. Heiser, J. P. Schunck, and A. Kempf, Influence of light on interstitial copper in p-type silicon, *Applied Physics A* **80**, 201–204 (2005).

[12] M. Boehringer, J. Hauber, S. Passefort, and K. Eason, In-line copper contamination monitoring using noncontact Q-SPV techniques, *Journal of the Electrochemical Society* **152**, G1–G6 (2005).

[13] J. Schmidt, K. Bothe, and R. Hezel, Formation and annihilation of the metastable defect in boron-doped Czochralski silicon, in *Proceedings of the 29th IEEE Photovoltaic Specialists Conference*, (Anchorage, AK, USA, 2002), pp. 178–181.

[14] K. Ramspeck, S. Zimmermann, H. Nagel, A. Metz, Y. Gassenbauer, B. Birkmann, and A. Seidl, Light induced degradation of rear passivated mc-Si solar cells, in *Proceedings of 27th European Photovoltaic Solar Energy Conference and Exhibition*, (Frankfurt, Germany, 2012), pp. 861–865.

[15] H. Fischer and W. Pschunder, Investigation of photon and thermal induced changes in silicon solar cells, in *Proceedings of 10th IEEE Photovoltaic Specialst Conference*, (Palo Alto, CA, USA, 1973), pp. 404–411.

[16] S. W. Glunz, S. Rein, W. Warta, J. Knobloch, and W. Wettling, Degradation of carrier lifetime in Cz silicon solar cells, *Solar Energy Materials & Solar Cells* **65**, 219–229 (2001).

[17] C. Möller and K. Lauer, Light-induced degradation in indium-doped silicon, *Physica Status Solidi RRL* **7**, 461–464 (2013).

[18] C. Möller and K. Lauer, ASi-Sii-defect model of light-induced degradation in silicon, *Energy Procedia* **55**, 559–563 (2014).

[19] S. Pingel, D. Koshnicharov, O. Frank, T. Geipel, Y. Zemen, B. Striner, and J. Berghold, Initial degradation of industrial silicon solar cells in solar panels, in *Proceedings of the 25th European Photovoltaic Solar Energy Conference and Exhibition*, (Valencia, Spain, 2010), pp. 4027–4032.

[20] V. Parra, T. Carballo, D. Cancillo, B. Moralejo, O. Martinez, J. Jimenez, J. Bullon, J. M. Miguez, and R. Ordas, Trends in crystalline silicon growth for low cost and efficient photovoltaic cells, in *Proceedings of the 2013 Spanish Conference on Electron Devices (CDE)*, (Valladolid, Spain, 2013), pp. 305–308.

[21] F. Fertig, K. Krauß, I. Geisemeyer, J. Broisch, H. Höffler, J. O. Odden, A.-K. Soiland, and S. Rein, Fully solderable large-area screen-printed Al-BSF p-type mc-Si solar cells from 100 % solar grade feedstock yielding $\eta > 17$ %: Challenges and potential on cell and module level, in *Proceedings of the 27th European Photovoltaic Solar Energy Conference and Exhibition*, (Frankfurt, Germany, 2012), pp. 1031–1038.

[22] W. Shockley and W. T. Read, Statistics of the recombinations of holes and electrons, *Physical Review* **87**, 835–842 (1952).

[23] R. N. Hall, Electron-hole recombination in germanium, *Physical Review* **87**, 387 (1952).

[24] D. K. Schroder, Carrier lifetimes in silicon, *IEEE Transactions on Electron* **44**, 160–170 (1997).

[25] S. K. Estreicher, Rich chemistry of copper in crystalline silicon, *Physical Review B* **60**, 5375–5382 (1999).

[26] A. A. Istratov, C. Flink, H. Heislmair, E. R. Weber, and T. Heiser, Intrinsic diffusion coefficient of interstitial copper in silicon, *Physical Review Letters* **81**, 1243–1246 (1998).

[27] S. K. Estreicher, D. J. Backlund, C. Carbogno, and M. Scheffler, Activation energies for diffusion of defects in silicon: The role of the exchange-correlation functional, *Angewandte Chemie, International Edition* **50**, 10221–10225 (2011).

[28] G. Mills and H. Jonsson, Quantum and thermal effects in H2 dissociative adsorption: Evaluation of free energy barriers in multidimensional quantum systems, *Physical Review Letters* **72**, 1124–1128 (1994).

[29] H. Jonsson, G. Mills, and K. W. Jacobsen, Nudged elastic band method for finding minimum energy paths of transitions, in *Classical and Quantum Dynamics in Condensed Phase Simulations*, edited by B. J. Berne, G. Ciccotti, and D. F. Coker, (World Scientific, Singapore, 1998), pp. 385–404.

[30] G. Henkelman, B. P. Uberuaga, and H. Jonsson, A climbing image nudged elastic band method for finding saddle points and minimum energy paths, *Journal of Chemical Physics* **113**, 9901–9904 (2000).

[31] G. Henkelman and H. Jonsson, Improved tangent estimate in the nudged elastic band method for finding minimum energy paths and saddle points, *Journal of Chemical Physics* **113**, 9978–9985 (2000).

[32] P. Wagner, H. Hage, H. Prigge, T. Prescha, and J. Weber, Properties of copper-induced complexes in silicon, in *Semiconductor Silicon-1990*, edited by H. R. Huff, K. G. Barraclough, and J.-I. Chikawa, (The Electrochemical Society, Pennington, NJ, 1990), pp. 675–686.

[33] H. Prigge, P. Gerlach, P. O. Hahn, A. Schnegg, and H. Jacob, Acceptor compensation in silicon induced by chemomechanical polishing, *Journal of the Electrochemical Society* **138**, 1385–1389 (1991).

[34] M. Miyazaki, *Recombination Lifetime Measurements in Silicon*, (ASTM, West Conshohockens, PA, 1998), pp. 294-304.

[35] J.-G. Lee and S. R. Morrison, Copper passivation of dislocations in silicon, *Journal of Applied Physics* **64**, 6679–6683 (1988).

[36] S. Naito and T. Nakashizu, Electric degradation and defect formation of silicon due to Cu, Fe, and Ni contamination, in *Defect Engineering in Semiconductor Growth, Processing and Device Technology*, (Materials Research Society, 1992), vol. 262, pp. 641–652.

[37] R. Sachdeva, A. A. Istratov, and E. R. Weber, Recombination activity of copper in silicon, *Applied Physics Letters* **79**, 2937–2939 (2001).

[38] A. A. Istratov, H. Heislmair, C. Flink, T. Heiser, and E. R. Weber, Interstitial copper-related center in n-type silicon, *Applied Physics Letters* **71**, 2349–2351 (1997).

[39] T. Heiser, A. Belayachi, and J. P. Schunck, Copper behavior in bulk silicon and associated characterization techniques, *Journal of the Electrochemical Society* **150**, G831–G837 (2003).

[40] C. Flink, H. Feick, S. A. McHugo, W. Seifert, H. Hieslmair, T. Heiser, A. A. Istratov, and E. R. Weber, Out-diffusion and precipitation of copper in silicon: An electrostatic model, *Physical Review Letters* **85**, 4900–4903 (2000).

[41] M. B. Shabani, S. Okuuchi, and Y. Shimanuki, Kinetics of low-temperature out-diffusion of copper from silicon wafers, in *Analytical and Diagnostic Techniques for Semiconductor Materials, Devices, and Processes*, edited by B. O. Kolbesen, C. Claeys, P. Stallhofer, F. Tardif, J. Benton, T. Shaffner, D. Schroder, S. Kishino, and P. Rai-Choudhury, (The Electrochemical Society, Pennington, NJ, 1999), vol. 99-16, pp. 510–525.

[42] M. B. Shabani, T. Yoshimi, and H. Abe, Low-temperature out-diffusion of Cu from silicon wafers, *Journal of the Electrochemical Society* **143**, 2025–2029 (1996).

[43] S. K. Estreicher, D. West, and P. Ordejon, Copper-defect and copper-impurity interactions in silicon, *Solid State Phenomena* **82-84**, 341–347 (2002).

[44] D. West and S. K. Estreicher, Copper interactions with H, O, and the self-interstitial in silicon, *Physical Review B* **68**, 035210 (2003).

[45] V. P. Markevich, A. R. Peaker, I. F. Medvedeva, V. E. Gusakov, L. I. Murin, and B. G. Svensson, Radiation-induced defect reactions in Cz-Si crystals contaminated with Cu, *Solid State Phenomena* **131-133**, 363–368 (2007).

[46] H. Lemke, Properties of copper donor levels in silicon, *Physica Status Solidi A* **1**, 283–286 (1970).

[47] M. M. Akhmedova, L. S. Berman, L. S. Kostina, and A. A. Lebedev, Investigation of parameters of copper levels in silicon by capacitance methods, *Soviet Physics Semiconductors USSR* **10**, 1400–1401 (1976).

[48] L. C. Kimerling, J. L. Benton, and J. J. Rubin, Transition metal impurities in silicon, in *Defects and radiation effects in semiconductors 1980*, edited by R. Hasiguti, (Institute of Physics, 1981), vol. 59 of *Inst. Phys. Conf. Ser.*, pp. 217–222.

[49] S. J. Pearton and A. J. Tavendale, Electrical properties of deep copper- and nickel-related centers in silicon, *Journal of Applied Physics* **54**, 1375–1379 (1983).

[50] H. Lemke, Defect reactions in Cu-doped silicon-crystals, *Physica Status Solidi A* **95**, 665–677 (1986).

[51] S. D. Brotherton, J. R. Ayres, A. Gill, H. W. Van Kesteren, and F. J. A. M. Greidanus, Deep levels of copper in silicon, *Journal of Applied Physics* **62**, 1826–1832 (1987).

[52] A. Mesli and T. Heiser, Defect reactions in copper-diffused and quenched p-type silicon, *Physical Review B* **45**, 11632–11641 (1992).

[53] H. Lemke, Substitutional transition metal defects in silicon grown-in by the float zone technique, in *Defects in Semiconductors*, edited by M. Suezawa and H. Katayama-Yoshida, (Materials Science Forum, 1995), vol. 196-201, pp. 683–688.

[54] M. Saritas and A. R. Peaker, Deep states associated with oxidation-induced stacking-faults in RTA p-type silicon before and after copper diffusion, *Solid-State Electronics* **38**, 1025–1034 (1995).

[55] K.-M. Chen and G.-G. Qin, Cu-related deep levels in Si and the interaction between Cu and irradiation defects, in *Defects in Semiconductors*, edited by H. von Bardeleben, (Materials Science Forum, 1986), vol. 10-12, pp. 1093–1098.

[56] A. A. Istratov and E. R. Weber, Electrical properties and recombination activity of copper, nickel and cobalt in silicon, *Applied Physics A* **66**, 123–136 (1998).

[57] M. Nakamura, S. Murakami, N. J. Kawa, S. Saito, K. Matsukawa, and H. Arie, Compositional transformation between Cu centers by annealing in Cu-diffused silicon crystals studied with deep-level transient spectroscopy and photoluminescence, *Japanese Journal of Applied Physics* **48**, 082302 (2009).

[58] A. A. Istratov, H. Hedemann, M. Seibt, O. F. Vyvenko, W. Schröter, T. Heiser, C. Flink, H. Hieslmair, and E. R. Weber, Electrical and recombination properties of copper-silicide precipitates in silicon, *Journal of the Electrochemical Society* **145**, 3889–3898 (1998).

[59] W. Schröter, V. Kveder, M. Seibt, H. Ewe, H. Hedemann, F. Riedel, and A. Sattler, Atomic structure and electronic states of nickel and copper silicides in silicon, *Materials Science & Engineering B* **72**, 80–86 (2000).

[60] D. Macdonald, A. Cuevas, S. Rein, P. Lichtner, and S. W. Glunz, Temperature- and injection-dependent lifetime spectroscopy of copper-related defects in silicon, in *Proceedings of the 3rd World Conference on Photovoltaic Energy Conversion*, (Osaka, Japan, 2003), pp. 87–90.

[61] S. Knack, J. Weber, H. Lemke, and H. Riemann, Copper-hydrogen complexes in silicon, *Physical Review B* **65**, 165203 (2002).

[62] J. Weber, L. Scheffler, V. Kolkovski, and N. Yarykin, New results on the electrical activity of 3d-transition metal impurities in silicon, *Solid State Phenomena* **205-206**, 245–254 (2014).

[63] A. Mesli, T. Heiser, and E. Mulheim, Copper diffusivity in silicon: A re-examination, *Materials Science & Engineering B* **25**, 141–146 (1994).

[64] J. Weber, H. Bauch, and R. Sauer, Optical properties of copper in silicon: Excitons bound to isoelectronic copper pairs, *Physical Review B* **25**, 7688–7699 (1982).

[65] P. N. Hai, T. Gregorkiewicz, C. A. J. Ammerlaan, and D. T. Don, Copper-related defects in silicon: Electron-paramagnetic-resonance identification, *Physical Review B* **56**, 4620–4625 (1997).

[66] M. L. W. Thewalt, M. Steger, A. Yang, N. Stavrias, M. Cardona, H. Riemann, N. V. Abrosimov, M. F. Churbanov, A. V. Gusev, A. D. Bulanov, I. D. Kovalev, A. K. Kaliteevskii, O. N. Godisov, P. Becker, H.-J. Pohl, J. W. Ager, and E. E. Haller, Can highly enriched 28Si reveal new things about old defects?, *Physica B* **401**, 587–592 (2007).

[67] M. Steger, A. Yang, N. Stavrias, M. L. W. Thewalt, H. Riemann, N. V. Abrosimov, M. F. Churbanov, A. V. Gusev, A. D. Bulanov, I. D. Kovalev, A. K. Kaliteevskii, O. N. Godisov, P. Becker, and H.-J. Pohl, Reduction of the linewidths

of deep luminescence centers in 28Si reveals fingerprints of the isotope constituents, *Physical Review Letters* **100**, 177402 (2008).

[68] K. Shirai, H. Yamaguchi, A. Yanase, and H. Katayama-Yoshida, A new structure of Cu complex in Si and its photoluminescence, *Journal of Physics: Condensed Matter* **21**, 06429 (2009).

[69] S. K. Estreicher and A. Carvalho, The CuPL defect and the Cus1Cui3 complex, *Physica B* **407**, 2967–2969 (2012).

[70] J. Weber, H. Bauch, and R. Sauer, Optical properties of copper in silicon: Excitons bound to isoelectronic copper pairs, *Physical Review B* **25**, 7688 (1982).

[71] M. Nakamura, Long-time stability of high-concentration copper complexes in silicon crystals, *Applied Physics Letters* **79**, 2904–2906 (2001).

[72] M. Nakamura and H. Iwasaki, Copper complexes in silicon, *Journal of Applied Physics* **86**, 5372–5375 (1999).

[73] S. Koveshnikov, Y. Pan, and H. C. Mollenkopf, Investigation of electronic states in copper doped p-type silicon, in *Proceedings of the Fourth International Symposium on High Purity Silicon*, edited by C. L. Claeys, P. Rai-Choudhury, P. Stallhofer, and J. E. Maurits, (The Electrochemical Society, Pennington, NJ, 1996), pp. 473–480.

[74] J. K. Solberg, Crystal-structure of η-Cu3Si precipitates in silicon, *Acta Crystallographica, Section A* **34**, 684–698 (1978).

[75] H. Gottschalk, Precipitation of copper silicide on glide dislocations in silicon at low-temperature, *Physica Status Solidi A* **137**, 447–461 (1993).

[76] M. Seibt and W. Schröter, Formation and properties of metastable silicide precipitates in silicon, *Solid State Phenomena* **19**, 283–294 (1991).

[77] M. Seibt and K. Graff, Characterization of haze-forming precipitates in silicon, *Journal of Applied Physics* **63**, 4444–4450 (1988).

[78] M. Seibt, R. Khalil, V. Kveder, and W. Schröter, Electronic states at dislocations and metal silicide precipitates in crystalline silicon and their role in solar cell materials, *Applied Physics A* **96**, 235–253 (2009).

[79] W. Schröter, M. Seibt, and D. Gilles, *Materials Science and Technology: A Comprehensive Teatment*, (VCH, New York, 1991).

[80] A. A. Istratov and E. R. Weber, Physics of copper in silicon, *Journal of the Electrochemical Society* **149**, G21–G30 (2002).

[81] M. Seibt, M. Greiss, A. A. Istratov, H. Hedemann, A. Sattler, and W. Schröter, Formation and properties of copper silicide precipitates in silicon, *Physica Status Solidi A* **166**, 171–182 (1998).

[82] M. Seibt, H. Hedemann, A. A. Istratov, F. Riedel, A. Sattler, and W. Schröter, Structural and electrical properties of metal silicide precipitates in silicon, *Physica Status Solidi A* **171**, 301–310 (1999).

[83] M. Seibt, Homogeneous and heterogeneous precipitation of copper in silicon, in *Semiconductor Silicon-1990*, edited by H. R. Huff, K. G. Barraclough, and J.-I. Chikawa, (The Electrochemical Society, Pennington, NJ, 1990), pp. 663–674.

[84] T. Buonassisi, M. D. Pickett, A. A. Istratov, E. Sauar, T. C. Lommasson, E. S. Marstein, T. Pernau, R. F. Clark, S. Narayanan, S. M. Heald, and E. R. Weber, Interactions between metals and different grain boundary types and their impact on multicrystalline silicon device performance, in *Proceedings of the 4th World Conference on Photovoltaic Energy Conversion*, (IEEE, Waikoloa, HI, USA, 2006), pp. 944–947.

[85] S. A. McHugo, A. Mohammed, A. C. Thompson, B. Lai, and Z. Cai, Copper precipitates in silicon: Precipitation, dissolution, and chemical state, *Journal of Applied Physics* **91**, 6396–6405 (2002).

[86] S. A. McHugo, Release of metal impurities from structural defects in polycrystalline silicon, *Applied Physics Letters* **71**, 1984–1986 (1997).

[87] S. A. McHugo and C. Flink, Thermal stability of copper precipitates in silicon, *Applied Physics Letters* **77**, 3598–3600 (2000).

[88] E. R. Weber, Impurity precipitation, dissolution, gettering, and passivation in PV silicon, Tech. Rep. NREL/SR-520-31528, National Renewable Energy Laboratory (2002).

[89] T. Heiser, S. McHugo, H. Hieslmair, and E. R. Weber, Transient ion drift detection of low level copper contamination in silicon, *Applied Physics Letters* **70**, 3576–3578 (1997).

[90] T. Heiser and A. Mesli, Determination of the copper diffusion coefficient in silicon from transient ion drift, *Applied Physics A* **57**, 325–328 (1993).

[91] D. A. Ramappa and W. B. Henley, Surface photovoltage analysis of copper in p-type silicon, *Applied Physics Letters* **72**, 2298–2300 (1998).

[92] A. A. Istratov, C. Flink, H. Heislmair, T. Heiser, and E. R. Weber, Influence of interstitial copper on diffusion length and lifetime of minority carriers in p-type silicon, *Applied Physics Letters* **71**, 2121–2123 (1997).

[93] R. R. Chromik, W. K. Neils, and E. J. Cotts, Thermodynamic and kinetic study of solid state reactions in the Cu-Si system, *Journal of Applied Physics* **86**, 4273–4281 (1999).

[94] A. Savchenkov, P. Shukrinov, P. Mutombo, J. Slezak, and V. Chab, Initial stages of Cu/Si interface formation, *Surface Science* **507-510**, 889–894 (2002).

[95] A. Cros, M. O. Aboelfotoh, and K. N. Tu, Formation, oxidation, electronic, and electrical properties of copper silicides, *Journal of Applied Physics* **67**, 3328 (1990).

[96] A. Sattler, H. Hedemann, A. A. Istratov, M. Seibt, and W. Schröter, The nature of the electronic states of Cu3Si-precipitates in silicon, *Solid State Phenomena* **63-4**, 369–374 (1998).

[97] M. Yoshida and K. Furusho, Behaviour of nickel as an impurity in silicon, *Japanese Journal of Applied Physics* **3**, 521–529 (1964).

[98] M. K. Bakhadyrkhanov, S. Zainabidinov, and A. Khamidov, Some characteristics of diffusion and electrotransport of nickel in silicon, *Soviet Physics Semiconductors USSR* **14**, 243 (1980).

[99] F. H. M. Spit, D. Gupta, and K. N. Tu, Diffusivity and solubility of Ni (63Ni) in monocrystalline Si, *Physical Review B* **39**, 1255–1260 (1989).

[100] V. A. Uskov, A. B. Fedotov, A. I. Rodionov, and N. S. Dumarevskaya, Interdiffusion and phase formation in the nickel silicon system, *Inorganic Materials* **20**, 7 (1984).

[101] R. D. Thompson, D. Gupta, and K. N. Tu, Low-temperature diffusion and solubility of Ni in P-doped Czochralski-grown Si, *Physical Review B* **33**, 2636–2641 (1985).

[102] J. W. T. Ridgway and D. Haneman, Diffusion of iron and nickel to silicon surfaces, *Physica Status Solidi* **38**, K31–K33 (1970).

[103] K. H. Yoon and L. L. Levenson, Diffusion kinetics of nickel in single-crystal silicon determined by in-depth Auger-electron spectroscopy, *Journal of Electronic Materials* **4**, 1249 (1975).

[104] G. L. P. Berning, K. H. Yoon, G. Lewis, S. Sinharoy, and L. L. Levenson, The observation of pseudodiffusion of nickel in single-crystal silicon by in-depth Auger electron spectroscopy, *Thin Solid Films* **45**, 141–145 (1977).

[105] D. J. Backlund and S. K. Estreicher, Ti, Fe, and Ni in Si and their interactions with the vacancy and the A center: A theoretical study, *Physical Review B* **81**, 235213 (2010).

[106] A. A. Istratov, P. Zhang, R. J. McDonald, A. R. Smith, M. Seacrist, J. Moreland, J. Shen, R. Wahlich, and E. R. Weber, Nickel solubility in intrinsic and doped silicon, *Journal of Applied Physics* **97**, 023505 (2005).

[107] H. Kitagawa, S. Tanaka, H. Nakashima, and M. Yoshida, Electrical properties of nickel in silicon, *Journal of Electronic Materials* **20**, 441–447 (1991).

[108] H. Lemke, Doping properties of nickel in silicium, *Physica Status Solidi A* **99**, 205–213 (1987).

[109] H. Kitagawa and H. Nakashima, Nickel-related deep levels in silicon studied by combined Hall-effect and DLTS measurement, *Physica Status Solidi A* **99**, K49–K52 (1987).

[110] H. Kitagawa and H. Nakashima, Nickel-related donor level in silicon, *Physica Status Solidi A* **102**, K23–K27 (1987).

[111] H. Kitagawa and S. Tanaka, Electrically active nickel in silicon studied by DLTS in several kinds of silicon diodes, *Physica Status Solidi A* **120**, K67–K70 (1990).

[112] S. K. Ghandi and F. L. Thiel, The properties of nickel in silicon, in *Proceedings of the IEEE*, (IEEE, 1969), vol. 57.

[113] G. P. Chiavarotti, M. Conti, and A. Messin, Characterisation of properties of nickel in silicon using thermally stimulated capacitance method, *Solid-State Electronics* **20**, 907–909 (1977).

[114] K. Graff and H. Pieper, Behaviour of transition and noble metals in silicon crystals, in *Semiconductor Silicon 1981*, (The Electrochemical Society, Minneapolis, MN, USA, 1981), vol. 81-5, pp. 331–343.

[115] M. Shiraishi, J.-U. Sachse, H. Lemke, and J. Weber, DLTS analysis of nickel-hydrogen complex defects in silicon, *Materials Science & Engineering B* **58**, 130–133 (1999).

[116] A. Tavendale and S. J. Pearton, Deep level, quenched-in defects in silicon doped with gold, silver, iron, copper or nickel, *Journal of Physics C* **16**, 1665–1673 (1983).

[117] J. Bartos and L. Tesar, Some electrical and optical-properties of nickel-related deep levels in silicon, *Physica Status Solidi A* **122**, 607–616 (1990).

[118] S. A. Azimov, N. A. Sultanov, L. Islamov, and R. N. Nagmatov, Infrared quenching of the photoconductivity of nickel-doped silicon, *Soviet Physics Semiconductors USSR* **7**, 1227–1228 (1974).

[119] H. Indusekhar and V. Kumar, Electrical properties of nickel-related deep levels in silicon, *Journal of Applied Physics* **61**, 1449–1455 (1987).

[120] P. Kaminski, R. Kozlowski, and A. Misiuk, Electrically active defects in Ni-contaminated Cz-Si with oxygen precipitates, in *Proceedings of SPIE - The International Society for Optical Engineering*, edited by B. W. Licznerski and A. Dziedzic, (Bellingham, WA, USA, 1996), vol. 2780, pp. 137–140.

[121] H. Kitagawa and H. Nakashima, Amphoteric property of electrically active nickel in silicon, *Japanese Journal of Applied Physics* **28**, 305–310 (1989).

[122] M. Gong and Z. P. You, The deep levels in nickel-doped silicon, *Physica Status Solidi A* **111**, K49–K52 (1989).

[123] M. Jaraiz, S. Duenas, J. Vicente, L. Bailon, and J. Barbolla, Electron thermal emission rates of nickel centers in silicon, *Solid-State Electronics* **29**, 883–884 (1986).

[124] W. B. Chua and K. Rose, Electrical properties of high-resistivity nickel-doped silicon, *Journal of Applied Physics* **41**, 2644–2647 (1970).

[125] S. Tanaka and H. Kitagawa, Distribution of electrically active nickel atoms in silicon crystals measured by means of deep level transient spectroscopy, *Physica B* **401-402**, 115–118 (2007).

[126] D. J. Backlund and S. K. Estreicher, Structural, electrical, and vibrational properties of Ti-H and Ni-H complexes in Si, *Physical Review B* **82**, 155208 (2010).

[127] T. Buonassisi, A. A. Istratov, M. D. Pickett, M. A. Marcus, G. Hahn, S. Riepe, J. Isenberg, W. Warta, G. Willeke, T. F. Ciszek, and E. R. Weber, Quantifying the effect of metal-rich precipitates on minority carrier diffusion length in multicrystalline silicon using synchrotron-based spectrally resolved X-ray beam-induced current, *Applied Physics Letters* **87**, 044101 (2005).

[128] M. Seibt and W. Schröter, Precipitation behavior of nickel in silicon, *Philosophical Magazine A* **59**, 337–352 (1989).

[129] C. Picker and P. S. Dobson, Precipitation of nickel in silicon, *Crystal Lattice Defects* **2**, 219–222 (1972).

[130] S. Sadamitsu, M. Sano, M. Hourai, S. Sumita, N. Fujino, and T. Shiraiwa, TEM observation of defects induced by Ni contamination on a Si(100) surface, *Japanese Journal of App* **28**, L333–L336 (1989).

[131] D. Walz, J. P. Joly, R. Falster, and G. Kamarinos, Characterization of nickel contamination in Float Zone and Czochralsky silicon wafers by using electrolytic metal tracer or microwave photoconductivity decay measurement, *Japanese Journal of Applied Physics* **34**, 4091–4095 (1995).

[132] M. B. Shabani, A quantitative method of metal impurities depth profiling for gettering evaluation in silicon wafers, *Solid State Phenomena* **57-58**, 81–90 (1997).

[133] Z. Xi, D. Yang, J. Chen, D. Que, and H. J. Moeller, Nickel precipitation in large-diameter Czochralski silicon, *Physica B* **344**, 407–412 (2004).

[134] H. Savin, M. Yli-Koski, A. Haarahiltunen, H. Talvitie, and J. Sinkkonen, Detection of nickel in silicon by recombination lifetime measurements, *Solid State Phenomena* **131-133**, 183–188 (2007).

[135] M. C. Schubert, H. Habenicht, and W. Warta, Imaging of metastable defects in silicon, *IEEE Journal of Photovoltaics* **1**, 168–173 (2011).

[136] J. Junge, A. Herguth, G. Hahn, D. Kreßner-Kiel, and R. Zierer, Investigation of degradation in solar cells from different mc-Si materials, *Energy Procedia* **8**, 52–57 (2011).

[137] V. V. Voronkov and R. Falster, Light-induced boron-oxygen recombination centers in silicon: Understanding their formation and elimination, *Solid State Phenomena* **205-206**, 3–14 (2014).

[138] J. Schmidt, A. A. Aberle, and R. Hezel, Investigation of carrier lifetime instabilities in Cz-grown silicon, in *Proceedings of 26th IEEE Photovoltaic Specialist Conference*, (Anaheim, CA, USA, 1997), pp. 13–18.

[139] V. V. Voronkov and R. Falster, Latent complexes of interstitial boron and oxygen dimers as a reason for degradation of silicon-based solar cells, *Journal of Applied Physics* **107**, 053509 (2010).

[140] H. Savin, M. Yli-Koski, and A. Haarahiltunen, Role of copper in light induced minority-carrier lifetime degradation of silicon, *Applied Physics Letters* **95**, 152111 (2009).

[141] G. Dingemans, P. Engelhart, R. Seguin, F. Einsele, B. Hoex, M. C. M. van den Sanden, and W. M. M. Kessels, Stability of Al2O3 and Al2O3/a-SiNx:H stacks for surface passivation of crystalline silicon, *Journal of Applied Physics* **106**, 114907 (2009).

[142] B. Liao, R. Stangl, T. Mueller, F. Lin, C. S. Bhatia, and B. Hoex, The effect of light soaking on crystalline silicon surface passivation by atomic layer deposited Al2O3, *Journal of Applied Physics* **113**, 024509 (2013).

[143] K. Bothe, J. Schmidt, and R. Hezel, Comprehensive analysis of the impact of boron and oxygen on the metastable defect in Cz silicon, in *Proceedings of the 3rd World Conference on Photovoltaic Energy Conversion*, (Osaka, Japan, 2003), pp. 1077–1080.

[144] J. Schmidt, K. Bothe, and R. Hezel, Structure and transformation of the metastable centre in Cz-silicon solar cells, in *Proceedings of the 3rd World Conference on Photovoltaic Energy Conversion*, (Osaka, Japan, 2003), pp. 2887–2892.

[145] H. Hashigami, M. Dhamrin, and T. Saitoh, Fast initial light-induced degradation of Czochralski silicon solar cells, in *Proceedings of the 3rd World Conference on Photovoltaic Energy Conversion*, (Osaka, Japan, 2003), pp. 1116–1119.

[146] T. U. Nærland, *Characterization of light induced degradation in crystalline silicon*, Ph.D. thesis, Norwegian University of Science and Technology, Trondheim (2013), 2013:303.

[147] J. Knobloch, S. W. Glunz, D. Biro, W. Warta, E. Schaffer, and W. Wettling, Solar cells with efficiencies above 21% processed from Czochralski grown silicon, in *Proceedings of 25th IEEE Photovoltaic Specialist Conference*, (Washington DC, USA, 1996), pp. 405–408.

[148] T. U. Nærland, H. Angelskår, M. Kirkengen, R. Søndenå, and E. S. Marstein, The role of excess carriers in light-induced degradation examined by photoluminescence imaging, *Journal of Applied Physics* **112**, 033703 (2012).

[149] K. Bothe, R. Hezel, and J. Schmidt, Recombination-enhanced formation of the metastable boron-oxygen complex in crystalline silicon, *Applied Physics Letters* **83**, 1125–1127 (2003).

[150] D. K. Schroder, *Semiconductor Material and Device Characterization*, (Wiley, 2006), 3rd ed.

[151] R. A. Sinton, A. Cuevas, and M. Stuckings, Quasi steady state photoconductance, a new method for solar cell material and device characterization, in *Proceedings of the 25th IEEE Photovoltaic Specialist Conference*, (IEEE, Washington, D.C., USA, 1996), pp. 457–460.

[152] D. W. Palmer, K. Bothe, and J. Schmidt, Kinetics of the electronically stimulated formation of a boron-oxygen complex in crystalline silicon, *Physical Review B* **76**, 035210 (2007).

[153] D. Macdonald, F. Rougieux, A. Cuevas, B. Lim, J. Schmidt, M. Di Sabatino, and L. J. Geerligs, Light-induced boron-oxygen defect generation in compensated p-type Czochralski silicon, *Journal of Applied Physics* **105**, 093704 (2009).

[154] K. Bothe and J. Schmidt, Electrically activated boron-oxygen-related recombination centers in crystalline silicon, *Journal of Applied Physics* **99**, 013701 (2006).

[155] S. Rein and S. W. Glunz, Electronic properties of the metastable defect in boron-doped Czochralski silicon: Unambiguous determination by advanced lifetime spectroscopy, *Applied Physics Letters* **82**, 1054–1056 (2003).

[156] J. Schmidt and A. Cuevas, Electronic properties of light-induced recombination centers in boron-doped Czochralski silicon, *Journal of Applied Physics* **86**, 3175–3180 (1999).

[157] M. Forster, E. Fourmond, F. E. Rougieux, A. Cuevas, R. Gotoh, K. Fujiwara, S. Uda, and M. Lemiti, Boron-oxygen defect in Czochralski-silicon co-doped with gallium and boron, *Applied Physics Letters* **100**, 042110 (2012).

[158] M. Forster, P. Wagner, J. Degoulange, R. Einhaus, G. Galbiati, F. Rougieux, A. Cuevas, and E. Fourmond, Impact of compensation on the boron and oxygen-related degradation of upgraded metallurgical-grade silicon solar cells, *Solar Energy Materials & Solar Cells* **120**, 390–395 (2014).

[159] R. Kopecek, J. Arumughan, K. Peter, E. A. Good, J. Libal, M. Acciarri, and S. Binetti, Crystalline Si solar cells from compensated material: Behaviour of light induced degradation, in *Proceedings of the 23rd European Photovoltaic Solar Energy Conference and Exhibition*, (Valencia, Spain, 2008), pp. 1855–1858.

[160] B. Lim, F. Rougieux, D. Macdonald, K. Bothe, and J. Schmidt, Generation and annihilation of boron-oxygen-related recombination centers in compensated p- and n-type silicon, *Journal of Applied Physics* **108**, 103722 (2010).

[161] K. Bothe, J. Schmidt, and R. Hezel, Effective reduction of the metastable defect concentration in boron-doped Czochralski silicon for solar cells, in *Proceedings of the 29th IEEE Photovoltaic Specialists Conference*, (IEEE, New Orleans, LA, USA, 2002), pp. 194–197.

[162] V. V. Voronkov, R. Falster, K. Bothe, B. Lim, and J. Schmidt, Lifetime-degrading boron-oxygen centres in p-type and n-type compensated silicon, *Journal of Applied Physics* **110**, 063515 (2011).

[163] V. V. Voronkov, R. Falster, K. Bothe, and B. Lim, Light-induced lifetime degradation in boron-doped Czochralski silicon: Are oxygen dimers involved?, *Energy Procedia* **38**, 636–641 (2013).

[164] J. R. Davis, A. Rohatgi, R. H. Hopkins, P. D. Blais, P. Rai-Choudhury, J. R. McCormick, and H. C. Mollenkopf, Impurities in silicon solar cells, *IEEE Transactions on Electron Devices* **4**, 677–687 (1980).

[165] J. Schmidt, Temperature- and injection-dependent lifetime spectroscopy for the characterization of defect centers in semiconductors, *Applied Physics Letters* **82**, 2178–2180 (2003).

[166] P. Rosenits, T. Roth, S. W. Glunz, and S. Beljakowa, Determining the defect parameters of the deep aluminum-related defect center in silicon, *Applied Physics Letter* **91**, 122109 (2007).

[167] S. W. Glunz, S. Rein, J. Knobloch, W. Wettling, and T. Abe, Comparison of boron- and gallium-doped p-type Czochralski silicon for photovoltaic application, *Progress in Photovoltaics* **7**, 463–469 (1999).

[168] F. A. Trumbore, Solid solubilities of impurity elements in germanium and silicon, *Bell System Technical Journal* **39**, 205–233 (1960).

[169] S. W. Glunz, S. Rein, W. Warta, J. Knobloch, and W. Wettling, On the degradation of Cz-silicon solar cells, in *Proceedings of the 2nd World Conference and Exhibition on Photovoltaic Solar Energy Conversion*, (Vienna, Austria, 1998), pp. 1343–1346.

[170] A. Herguth, G. Schubert, M. Kaes, and G. Hahn, A new approach to prevent the negative impact of the metastable defect in boron doped Cz silicon solar cells, in *Proceedings of the 4th World Conference on Photovoltaic Energy Conversion*, (IEEE, Waikoloa, HI, USA, 2006), pp. 940–943.

[171] A. Herguth, G. Schubert, M. Kaes, and G. Hahn, Investigations on the long time behavior of the metastable boron-oxygen complex in crystalline silicon, *Progress in Photovoltaics* **16**, 135–140 (2008).

[172] B. Lim, K. Bothe, and J. Schmidt, Deactivation of the boron-oxygen recombination center in silicon by illumination at elevated temperature, *Physica Status Solidi RRL* **2**, 93–95 (2008).

[173] B. Lim, A. Liu, D. Macdonald, K. Bothe, and J. Schmidt, Impact of dopant compensation on the deactivation of boron-oxygen recombination centers in crystalline silicon, *Applied Physics Letters* **95**, 232109 (2009).

[174] B. Lim, K. Bothe, and J. Schmidt, Impact of oxygen on the permanent deactivation of boron-oxygen-related recombination centers in crystalline silicon, *Journal of Applied Physics* **107**, 123707 (2010).

[175] K. A. Münzer, Hydrogenated silicon nitride for regeneration of light induced degradation, in *Proceedings of the 24th European Photovoltaic Solar Energy Conference*, (Hamburg, Germany, 2009), pp. 1558–1561.

[176] S. Wilking, A. Herguth, and G. Hahn, Influence of hydrogen on the regeneration of boron-oxygen related defects in crystalline silicon, *Journal of Applied Physics* **113**, 194503 (2013).

[177] H. Nagel, J. Schmidt, A. A. Aberle, and R. Hezel, Exceptionally high bulk minority-carrier lifetimes in block-cast multicrystalline silicon, in *Proceedings of the 14th European Photovoltaic Solar Energy Conference*, (Barcelona, Spain, 1997), pp. 762–765.

[178] D. Macdonald, L. J. Geerligs, and S. Riepe, Light-induced lifetime degradation in multicrystalline silicon, in *Proceedings of the 13th Workshop on Crystalline Silicon Solar Cell Materials and Processes*, (Vail, CO, USA, 2003), pp. 182–185.

[179] G. Coletti, C. L. Mulder, G. Galbiati, and L. J. Geerligs, Reduced effect of B-O degradation on multicrystalline silicon wafers, in *Proceedings of the 21st European Photovoltaic Energy Conference and Exhibition*, (Dresden, Germany, 2006), pp. 1515–1518.

[180] S. Dubois, N. Enjalbert, J. Veirman, J. P. Garandet, F. Tanay, A. Jouini, and J. Champliaud, Evidences on the carbon participation for the slowing down of the boron-oxygen defects activation kinetics in solar-grade silicon, in *Proceedings of 6th International Workshop on Science and Technology of Crystalline Silicon Solar Cells*, (Aix-les-Bains, France, 2012).

[181] J. Safarian, G. Tranella, and M. Tangstada, Processes for upgrading metallurgical grade silicon to solar grade silicon, *Energy Procedia* **20**, 88–97 (2012).

[182] I. Tarasov, S. Ostapenko, and S. S. Koveshnikov, Light induced defect reactions in boron-doped silicon: Cu versus Fe, in *Proceedings of 8th Workshop on Crystalline Silicon Solar Cell Materials and Process*, (Copper Mountain, CO, USA, 1998), pp. 207–210.

[183] H. Väinölä, E. Saarnilehto, M. Yli-Koski, A. Haarahiltunen, J. Sinkkonen, G. Berenyi, and T. Pavelka, Quantitative copper measurement in oxidized p-type silicon wafers using microwave photoconductivity decay, *Applied Physics Letters* **87**, 032109 (2005).

[184] M. Yli-Koski, H. Väinölä, A. Haarahiltunen, J. Storgårds, E. Saarnilehto, and J. Sinkkonen, Light activated copper defects in p-type silicon studied by PCD, *Physica Scripta T* **T114**, 69–72 (2004).

[185] M. Yli-Koski, *Optical activation of copper in silicon studied by carrier lifetime measurements*, Ph.D. thesis, Helsinki University of Technology (2004).

[186] D. P. Fenning, A. S. Zuschlag, M. I. Bertoni, B. Lai, G. Hahn, and T. Buonassisi, Improved iron gettering of contaminated multicrystalline silicon by high-temperature phosphorus diffusion, *Journal of Applied Physics* **113**, 214504 (2013).

[187] D. Macdonald, A. Cuevas, A. Kinomura, and Y. Nakano, Phosphorus gettering in multicrystalline silicon studied by neutron activation analysis, in *Proceedings of the 29th IEEE Photovoltaic Specialist Conference*, (IEEE, New Orleans, LA, USA, 2002), pp. 285–288.

[188] A. Bentzen, A. Holt, R. Kopecek, G. Stokkan, J. S. Christensen, and B. G. Svensson, Gettering of transition metal impurities during phosphorus emitter diffusion in multicrystalline silicon solar cell processing, *Journal of Applied Physics* **99**, 093509 (2006).

[189] F. S. Ham, Theory of diffusion-limited precipitation, *Journal of Physics and Chemistry of Solids* **6**, 335–351 (1958).

[190] M. Yli-Koski, M. Palokangas, A. Haarahiltunen, H. Väinölä, J. Storgårds, H. Holmberg, and J. Sinkkonen, Detection of low-level copper contamination in p-type silicon by means of microwave photoconductive decay measurements, *Journal of Physics Condensed Matter* **14**, 13119–13125 (2002).

[191] L. Fabry, R. Hoelzl, A. Andrukhiv, K. Matsumoto, J. Qiu, S. Koveshnikov, M. Goldstein, A. Grabau, H. Horie, and R. Takeda, Test methods for measuring bulk copper and nickel in heavily doped p-type silicon wafers, *Journal of the Electrochemical Society* **153**, G566–G571 (2006).

[192] Y. Kitagawara, H. Takeno, S. Tobe, Y. Hayam Izu, T. Koide, and T. Takenaka, Systematic analyses of practical problems related to defects and metallic impurities in silicon, in *Materials Research Society Symposium Proceedings*, edited by S. Ashok, J. Chevallier, W. Goetz, B. L. Sopori, and K. Sumino, (Materials Research Society, 1998), vol. 510, pp. 3–14.

[193] R. Hoelzl, D. Huber, K.-J. Range, L. Fabry, J. Hage, and R. Wahlich, Gettering of copper and nickel in p/p+ epitaxial wafers, *Journal of the Electrochemical Society* **147**, 2704–2710 (2000).

[194] R. Hoelzl, K.-J. Range, and L. Fabry, Modeling of Cu gettering in p- and n-type silicon and in poly-silicon, *Applied Physics A* **75**, 525–534 (2002).

[195] T. Buonassisi, M. A. Marcus, A. A. Istratov, M. Heuer, T. F. Ciszek, B. Lai, Z. Cai, and E. R. Weber, Analysis of copper-rich precipitates in silicon: Chemical state, gettering, and impact on multicrystalline silicon solar cell material, *Journal of Applied Physics* **97**, 063503 (2005).

[196] X.-Q. Li, D.-R. Yang, X.-G. Yu, and D.-L. Que, Precipitation and gettering behaviors of copper in multicrystalline silicon used for solar cells, *Transactions of Nonferrous Metals Society of China* **21**, 691–696 (2011).

[197] G. von Gastrow, S. Li, P. Repo, Y. Bao, M. Putkonen, and H. Savin, Ozone-based batch atomic layer deposited Al2O3 for effective surface passivation, *Energy Procedia* **38**, 890–894 (2013).

[198] H. Amjadi, The mechanism of voltage decay in corona-charged layers of silicon dioxide during UV irradiation, *IEEE Transactions on Dielectrics and Electrical Insulation* **7**, 222–228 (2002).

[199] L. E. Black and K. R. McIntosh, Defect generation at charge-passivated Si-SiO2 interfaces by ultraviolet light, *IEEE Transactions on Electron Devices* **57**, 1996–2004 (2010).

[200] R. Hezel and K. Jaeger, Low-temperature surface passivation of silicon for solar cells, *Journal of the Electrochemical Society* **136**, 518–523 (1989).

[201] G. Dingemans and W. M. M. Kessels, Status and prospects of Al2O3-based surface passivation schemes for silicon solar cells, *Journal of Vacuum Science & Technology A* **30**, 040802 (2012).

[202] V. Vähänissi, A. Haarahiltunen, H. Talvitie, M. Yli-Koski, and H. Savin, Impact of phosphorus gettering parameters and initial iron level on silicon solar cell properties, *Progress in Photovoltaics* **21**, 1127–1135 (2013).

[203] S. Bernardini, D. Saynova, S. Binetti, and G. Coletti, Light-induced degradation in compensated mc-Si p-type solar cells, in *Proceedings of the 38th IEEE Photovoltaic Specialists Conference*, (Austin, TX, USA, 2012), pp. 3242–3247.

Errata

Publication I

The bias light intensity was $18{-}25$ Wcm^{-2} instead of >25 Wcm^{-2}.

Publication II

The bias light intensity was $18{-}25$ Wcm^{-2} instead of >25 Wcm^{-2}. The positive corona charge density was $+0.78$ µCcm^{-2} instead of $+3.7$ µCcm^{-2}. The negative corona charge densities were -0.78 and -2.34 µCcm^{-2} instead of -3.7 and -11.1 µCcm^{-2}, respectively.

Publication V

The positive corona charge density was $+0.52$ µCcm^{-2} instead of $+4$ µCcm^{-2}. The negative corona charge densities were -1.3 and -1.7 µCcm^{-2} instead of -10 and -12.8 µCcm^{-2}, respectively. Therefore, the negative corona charge density in the top oxidized sample was -1.0×10^{13} cm^{-2} instead of -6.2×10^{13} cm^{-2}. In FIG. 5, the term *center* refers to the middle of the ingot.

Aalto-DD 37/2015

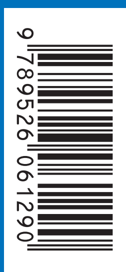

ISBN 978-952-60-6129-0 (printed)
ISBN 978-952-60-6130-6 (pdf)
ISSN-L 1799-4934
ISSN 1799-4934 (printed)
ISSN 1799-4942 (pdf)

Aalto University
School of Electrical Engineering
Department of Micro- and Nanosciences
www.aalto.fi

BUSINESS +
ECONOMY

ART +
DESIGN +
ARCHITECTURE

SCIENCE +
TECHNOLOGY

CROSSOVER

DOCTORAL
DISSERTATIONS